University of Southampton
Faculty of Engineering, Science and Mathematics
Institute of Sound and Vibration Research

Distortion Product Otoacoustic Emissions: Challenging Existing Theory

Richard John Perdue

A dissertation submitted in partial fulfilment of the requirements for the degree of Master of Science by taught course.

2010

ABSTRACT

Distortion product otoacoustic emissions (DPOAE or DP) are generated using two primary tones at frequencies f1 and f2 at levels L1 and L2; the two most prominent DP are cubic distortion products at the frequencies 2f1−f2 and 2f2−f1. Current understanding of their origin indicates that they arise via two distinct mechanisms. One mechanism is thought to be non-linear distortion and the other linear coherent reflection. Recent investigations have confirmed that both components are present in the 2f2−f1 DP, which conflicts with current understanding of the generation mechanisms, suggesting that the location of origin of the DP at 2f2−f1 may be different from that at 2f1−f2.

Distortion and reflection components of DP combine in the cochlea. One method to separate them is time window separation, which utilises phase variation in the frequency domain to infer latency in the time domain, by means of inverse Fourier transformation. It is independent of the location of generation of the DP but depends on the generation *mechanism*. By contrast, DP can be reduced by the introduction of a third suppressor tone, which can be used to infer the *location* of DP generation based of the suppressor tone frequency, independent of generation mechanism.

The aim of this investigation was to assess the effect of suppressor frequency and level on the 2f2−f1 DP, in order to make inferences about where this DP originates. Twenty normally hearing participants took part in the investigation. DP were measured (L1 = 65, L2 = 55 dB SPL) with a fixed frequency ratio f2/f1 = 1.05. By sweeping the primary frequencies in the ranges f2 = 1.75-2.25 and 3.75-4.25 kHz, suitable fixed test frequencies were identified for subsequent suppression testing in each ear, as the frequencies giving DP with the greatest signal-to-noise ratio. The frequency sweeps also allowed analysis by time window separation. Suppression was carried out with suppressor levels introduced at 0, 20, 40 and 60 dB SPL. The frequency of the suppressor was altered from −32 Hz to +64 Hz relative to the DP, in 16 Hz increments.

Results of time window separation confirmed that both non-linear distortion and reflection components were present in both the 2f2−f2 DP and 2f2−f1 DP. However, it was not possible to separate the two components of the 2f2−f1 DP by suppression, which suggests that the 2f2−f1 DP is not generated at a discrete place. It is concluded that the generation mechanism for the 2f2−f1 DP may be distributed along the cochlear partition at or basal to the characteristic place corresponding to the DP frequency.

DECLARATION

I, Richard John Perdue, declare that the thesis is my own work, except where acknowledged, and that the research reported in this thesis was conducted in accordance with the principles for the ethical treatment of human participants as approved for this research by the Ethics Committee at the Institute of Sound and Vibration Research, University of Southampton.

ACKNOWLEDGEMENTS

The author would like to thank all of the participants who contributed their time in order to be tested for this project. Thanks to Dr Ben Lineton for advice on calibration. Finally, thanks to Professor Mark E Lutman for his advice and guidance throughout the construction of this thesis.

CHAPTER 1: BACKGROUND

1.1 Introduction

1.1.1 Defining the issue

Regardless of the initial excitement concerning Kemp's (1978) revelation that the inner ear emits sounds for diagnostic utility in the clinic, otoacoustic emissions (OAEs) have advanced no further than being able to differentiate between 'normal' and 'impaired' auditory functioning (Shera, 2004). Otoacoustic emissions are used in the clinic environment, being especially important in the newborn hearing-screening programme. It is obvious that OAEs could be utilised in a far more helpful way, in order to give more frequency specific and detailed characterisation concerning the mechanisms of the middle and inner ear. Indeed, there is much evidence correlating behavioural thresholds in humans with OAE amplitude (Lonsbury-Martin and Martin, 1990; Gaskill and Brown, 1990). There is also the potential to use OAEs to monitor changes in the cochlea due to ototoxicity and exposure to loud sounds. Investigations of this clinical application in human ears have been hindered by the great range of results seen in the OAE amplitude of normal hearing humans (Gaskill and Brown, 1990; Suckfull et al., 1996).

In both major research areas concerning evoked OAEs, in a laboratory and clinical setting, the interpretation of measured OAE responses is dependent on the current understanding of their origins (Shera, 2004). Since their discovery various models have been developed in order to explain the mechanisms of generation of OAEs. By further understanding the generation mechanisms underlying OAEs we will be closer to enabling their full potential in both the laboratory and clinic setting.

1.1.2 Outline

In this chapter the literature concerning the experimental investigations and models that form the basis of current understanding of the mechanisms and sources of

distortion product OAEs (DPOAEs) are reviewed. The limitations of current practices are explored, and current gaps in knowledge are highlighted in order to emphasise further areas of research. This will aid in broadening the understanding of cochlear function, and help advance the clinical utility of DPOAEs.

The paper will begin by giving an overview of the mechanics of cochlear function. This will be followed by a description of recent advancements made in the understanding of the origin of OAEs, and the evolution of theory. Descriptions of experimental method and findings will be discussed relating to current interpretation, and criticised where appropriate. The referenced articles are grouped by topic. A methodology is then described and results presented. The results are then discussed and conclusions drawn. Areas of controversy and disagreement will be focussed upon and the paper will highlight gaps in current knowledge. Emphasis will then be placed on recommendations for future research.

1.2 The mechanics of cochlear function

In order to understand how OAEs are generated it is important to know detail of the physiological processes occurring in the cochlea.

1.2.1 The linear transformer and the basilar membrane

The significance of the outer ear and middle ear mechanisms in transferring sound energy to the inner ear is widely known (Hammershoi and Moller, 1996; Handel, 1989, page 64). The efficiency by which sound is transferred from the outer and middle ear to the inner ear is dependent upon how well the low acoustic impedance of air is coupled to the high impedance fluid filled cochlea (Kemp, 2002). The difference between the impedances of the fluid within the cochlea and the air is estimated to be 4000:1. The middle ear increases the level of mechanical force created by sound in the air, in order to correct for this difference in impedance values. The middle ear effectively acts as a linear transformer (Gelfand, 2007, page 89). Given values supplied by Gelfand (2007, page 94) using an effective area ratio of 26.6

(difference between the tympanic membrane and the oval window), an ear drum buckling factor of 2.0, and a ossicular lever ratio of 1.3, the human middle ear transformer ratio may be 69.2 to 1, corresponding to 36.8 dB. The real value is often less due to frequency effects and transmission losses. This results in greater cochlear fluid movement, which excites the sensory hair cells. Consequently the health of the middle ear has implications on OAEs and can interfere with their measurement.

Bekesy (1948, in Gelfand, 2007) demonstrated that there is a widening of the basilar membrane with increasing distance from the base to apex. The stimulation of the cochlea creates a travelling wave (TW). Oscillatory transfer takes place between the kinetic energy in the cochlea fluid and the elastic energy stored in basilar membrane (BM) movement. Basilar membrane segments located adjacent to one another gain energy as the fluid moves, for example, when the BM rises at a point it causes the adjacent less stiff apical point to move also, creating a TW (Kemp, 2002). Bekesy (1960) reported from investigations conducted on human cadavers that the elasticity of the cochlear partition changed by a factor of 100 from the base to the apex of the 35 mm cochlea (Emadi et al., 2004). There is an increasing widening, corresponding with a decrease in stiffness. This stiffness gradient effectively creates a series of low pass filters, meaning that peaks in the TW occur at the base for high frequencies and near the apex for low frequencies (Handel, 1989, page 64). Travelling waves move from the base to the apex (Gelfand, 2007, page 127).

1.2.2 The travelling wave

The displacement amplitude increases as the TW moves toward the apex, reaching a peak at the resonant frequency, beyond that the TW decays rapidly (Duke and Julicher, 2003; Moller, 1973). The TW peak occurs at the resonant frequency. The TW displacement patterns that Bekesy observed on the BM are characterised by three properties. 1) Displacements have greater phase lags with increasing distance from the oval window. 2) The sizes of displacements have an asymmetrical envelope around the characteristic place, with the apical slope having a greater gradient than the basal slope. 3) The TWs are the result of the passive mechanical characteristics of cochlear tissues and fluids (Robles and Ruggero, 2001).

The 'lost' energy is transferred to the organ of Corti, or dissipated in resistive elements.

The organ of Corti mechanism then converts BM motion into fluid motion across the inner hair cell (IHC) stereocilia, resulting in excitation of neurones. Forces exerted on the ciliary bundle derive from relative displacements between the reticular lamina and the tectorial membrane, either due to direct attachment of cilia or due to tectorial membrane driven flow of endolymph around the cilia (Dallos, 1992). A well-established theory of hair cell transduction highlights mechanically gated ion channels located at or near the tips of stereocilia. Bundle displacement toward the tallest cilia is excitory; movement in the opposite direction is inhibitory (Dallos, 1992). Gelfand (2007, page 148) explains that the cochlea is tuned to specific frequencies as a function of distance along the cochlea. This relationship is described by Liberman's (1982) cochlear frequency map (Gelfand, 2007). The ability to separate competing sounds of differing frequencies is a fundamental component of the auditory system (Oxenham and Shera, 2003).

1.2.3 The non-linear cochlear amplifier

Energy is lost within the cochlea due to viscous losses (Kemp, 2002). Absorption of energy is fundamental to the functioning of the sensory cells, in order to stimulate the IHCs. The movement of fluid occurs in the sub-tectorial space. This energy loss is compensated for by the 'cochlear amplifier' (Kemp, 2002). Bekesy's initial recordings of the TW in the dead ear implied linearity and shallow tuning. When it became possible to measure the BM response of living organisms, a significant difference from Bekesy's results was unveiled (Duke and Julicher, 2003). A rise in the energy present implied that energy is supplied to the TW in excess of that present in the eliciting stimulus. Calculations based on data from active cochlea suggest that BM vibrations are biologically amplified, in comparison to inactive cochlea (Robles and Ruggero, 2001). The system is shown to be non-linear with regard to stimulus level, and it is much more sharply tuned (Dallos, 1992). This is due to mechanical feedback produced by outer hair cells (OHCs).

Dallos (1992) discusses the fact that the mechanical nature of the active cochlear process is indicated by the detection of sound in the ear canal, OAEs. The cochlear amplifier results in increased vibratory stimulus being delivered to the IHCs, leads to the sharp cochlear tuning and non-linear responses, and creates OAEs. This arises as the OHCs rapidly contract and expand (up to 3-5%) in response to sound (Dallos, 1992).

OAEs are potentially located in the external ear as a consequence of the BM disturbances that are released from the amplifier mechanism toward the cochlear base (Kemp, 2002). The shifting movement of the BM creates a variation in oscillating fluid pressure on the oval and round windows. This leads to vibration of the ossicles and the drum, via a reverse TW. OAEs are only present in non-pathological ears; the cochlear amplifier must be functioning. Vibrations are sent back to the base to form OAEs due to spatial imperfections and also as some energy is released basally (this energy can be partially reflected back, resulting in repetitive circulation of the TW) (Kemp, 2002). In the case of uneven OHC movement, a stimulus frequency OAE (SFOAE) is created at the same frequency as the stimulus.

1.3 The non-linear distortion model

1.3.1 An integrated model of cochlear function

The non-linear distortion model theorises that when the cochlear response is non-linear the TW produces localised distortions, approximately around the TW peak. This is referred to as a wave-fixed phenomenon. DPOAEs were historically considered to be created directly as a result of this process, as this seemed to encompass the frequency dependence of cochlear TWs. This was thought to arise via the electromotile responses of OHCs (Shera and Guinan, 1999). DPOAEs were thought to arise through non-linear stimulus re-emission. Stimulus re-emission was thought to primarily occur at the peak of the TW envelope, resulting in the creation of backward TWs. DPOAEs occur as a result of non-linear distortion (Shera and

Guinan, 1999; Robinette and Glattke, 2007, page 32). This non-linear distortion can be seen in Figure. 1.1, which illustrates that as the frequency alters the wave moves. According to the integrated view DPOAEs were generated by non-linear distortion (Shera, 2004). In situations in which the cochlear map is logarithmic, the relative wavelengths of the TW are independent of frequency. A low frequency wave moves a greater distance and is slower in reaching its peak than a high frequency wave. The two TWs however travel the same number of wavelengths, and the phase accumulation is equal (Shera, 2004).

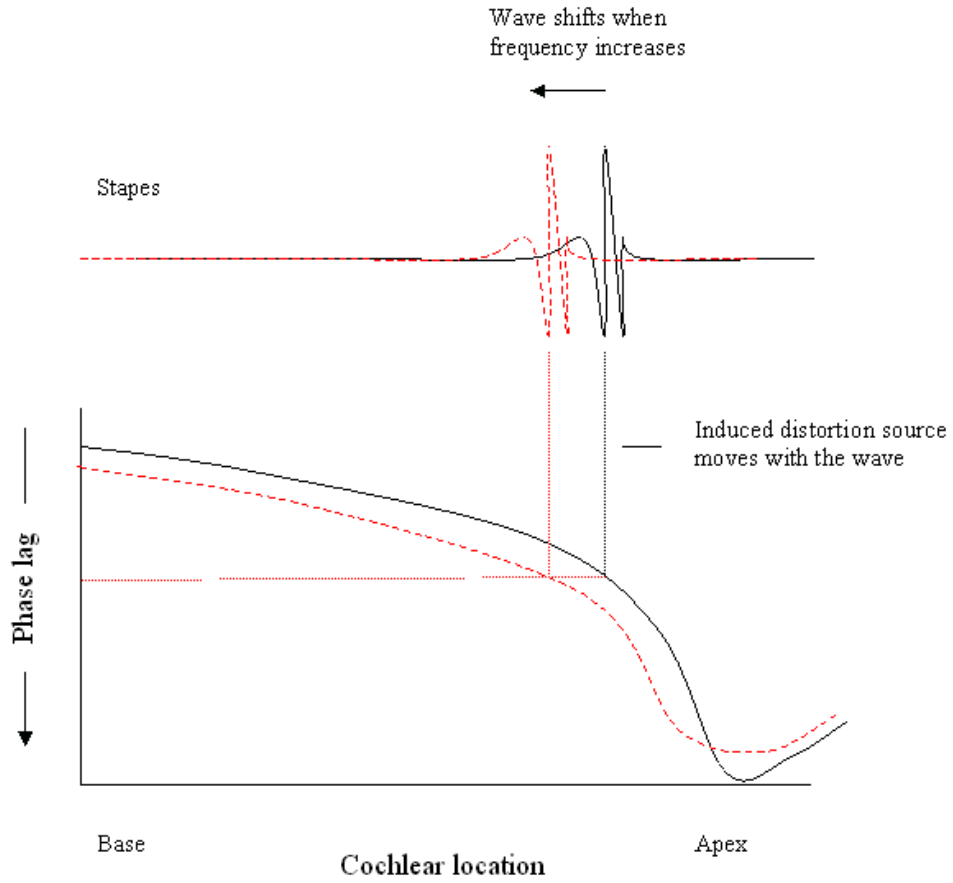

Figure 1.1 Diagrammatic representation of non-linear distortion for a pure-tone stimulus. The black line at the top illustrates a frozen image of the TW and the black line at the bottom shows the phase delay. As a result of the non-linearities in the cochlear mechanisms a TW leads to the creation of backward travelling waves. As this distortion source is a result of the wave itself, the phase of the wave at the source remains constant as the frequency is raised (grey line), with pattern moving toward the base. The amplitudes are exaggerated here for illustration purposes. Source: Shera, 2004, page 3.

According to this model, the emission phase is an accumulation of 1) wave travel toward and away from the site of re-emission and 2) from the non-linear re-emission process itself (Shera, 2004). Sources of non-linear distortion are induced by and move with the wave when the frequency is varied. This means that the phase lag experienced by the TW is independent of frequency (Shera, 2004).

DPOAEs are normally elicited by two prolonged pure tones with frequencies f1 and f2. These are referred to as primaries. According to convention the lower-frequency pure tone is labelled as the f1 primary, and its corresponding level as L1, and the higher-frequency primary is labelled as f2 (f2 > f1), and its corresponding level is L2 (Robinette and Glattke, 2007). The frequency separation of the primaries, the f2/f1 ratio is often 1.2. The most common distortion product frequency measured in the human ear is 2f1− f2, as in humans it is the greatest DPOAE (Figure. 1.2). The phases of f1 and f2 at any point on the BM are a consequence of the location of the point with respect to the TWs each stimulus creates (Robinette and Glattke, 2007). This emission is dependent on the wave characteristics of the stimulus TW. Moving the frequencies together will move the positions of the TW peaks but will not influence their spatial phase relationship (Robinette and Glattke, 2007).

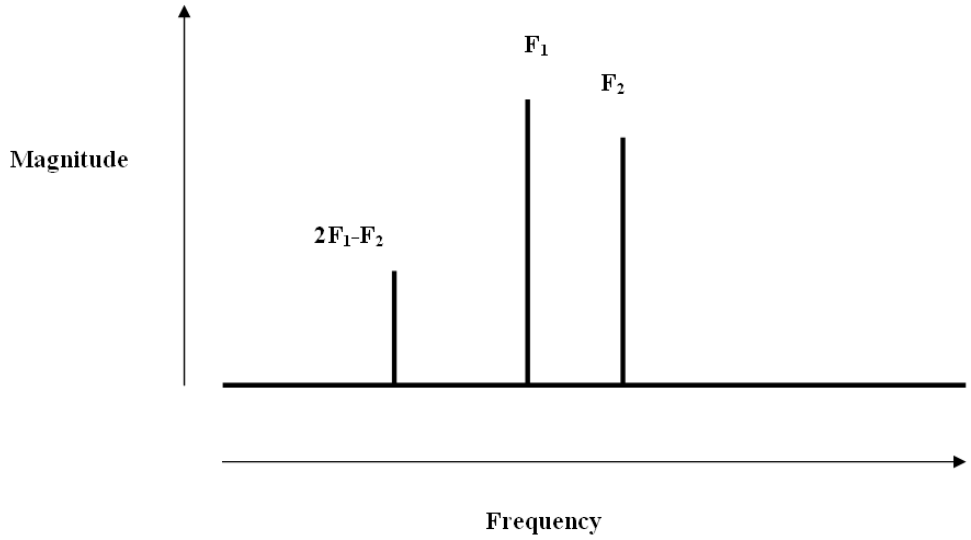

Figure 1.2 The most commonly observed DP is 2f1− f2. The diagram highlights the location of this DP relative to its eliciting primary tones (F1 and F2). The 2f1− f2 DP is the largest DP measurable. Source: Sharp, 2007.

From this model a constant phase is expected. Upon investigation this can be found, thus the model appears true for DPOAEs caused directly by distortion. However, SFOAE alter greatly so although the non-linear distortion model holds true for distortion products, it predicts a constant SFOAE and transient evoked OAE (TEOAE) in contrast to what is shown experimentally. Consequently pure DPOAE and low level SFOAE and TEOAE must arise by different mechanisms (Shera, 2004).

1.4 Mechanism based taxonomy

1.4.1 Non-linear distortion and linear reflection

Although the model proposed by Kemp (1978) is still relevant it is an over-simplification of the actual processes taking place (Shera and Guinan, 1999). The Kemp (1978) model is location based. It has since been suggested that OAEs are the result of two fundamentally different mechanisms. This mechanism-based taxonomy separates emissions into distortion and reflection emissions (Kalluri and Shera, 2001) (Figure. 1.3). The Shera and Guinan (1999) model implies that the reflection mechanism involves reflection of the distortion component travelling forward. This differs from the wave and place-fixed theories suggested by Kemp and Brown (1983) as this theory implied all OAEs were the result of non-linearity (Shera and Guinan, 1999). The primary TWs f1 and f2 (f2 > f1) interact to produce a non-linear distortion near the peak of f2, increasing energy at DP frequencies (Kalluri and Shera, 2001). Travelling waves at 2f1− f2 move in both the forward and reverse direction. The forward TW moves to its frequency place where partial reflections occur through a linear mechanism (Shera et al., 2004), creating a second backward TW that moves to the ear canal.

Reflections occur at random inhomogeneities located along the cochlear partition, fixed in location (Shaffer, 2003). Figure. 1.4 illustrates the phase of the wave changing with frequency at one of these perturbations. Examples of these

irregularities include differences in the quantity of hair cells or differences in their geometry, and irregularities in the anatomy such as in OHC forces resulting from variations in the number of motor proteins (Shera et al., 2004).

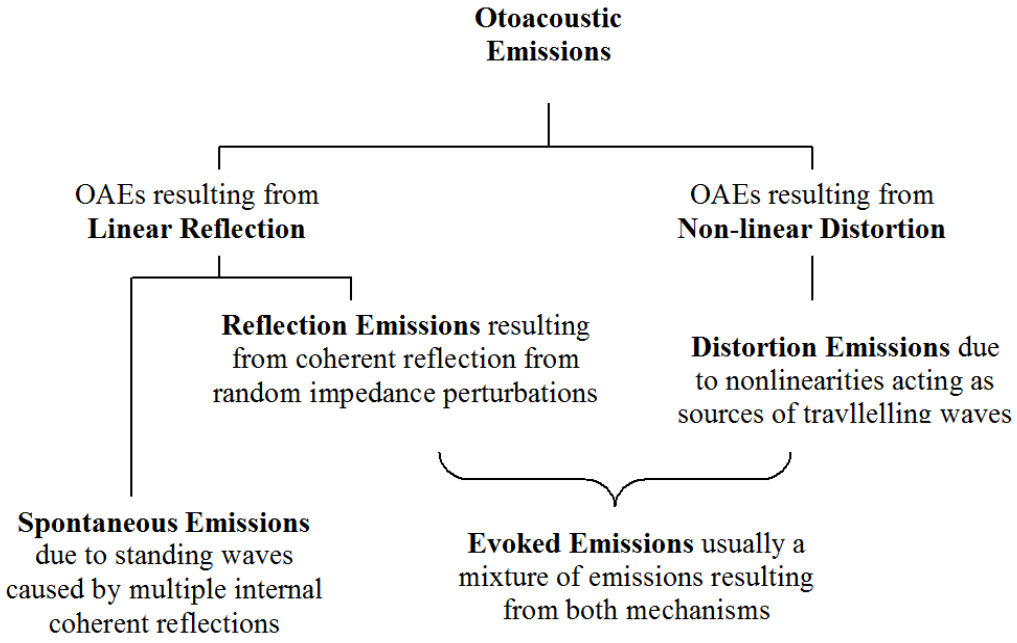

Figure 1.3 The mechanism based taxonomy for mammalian OAEs. Source: Shera, 2004.

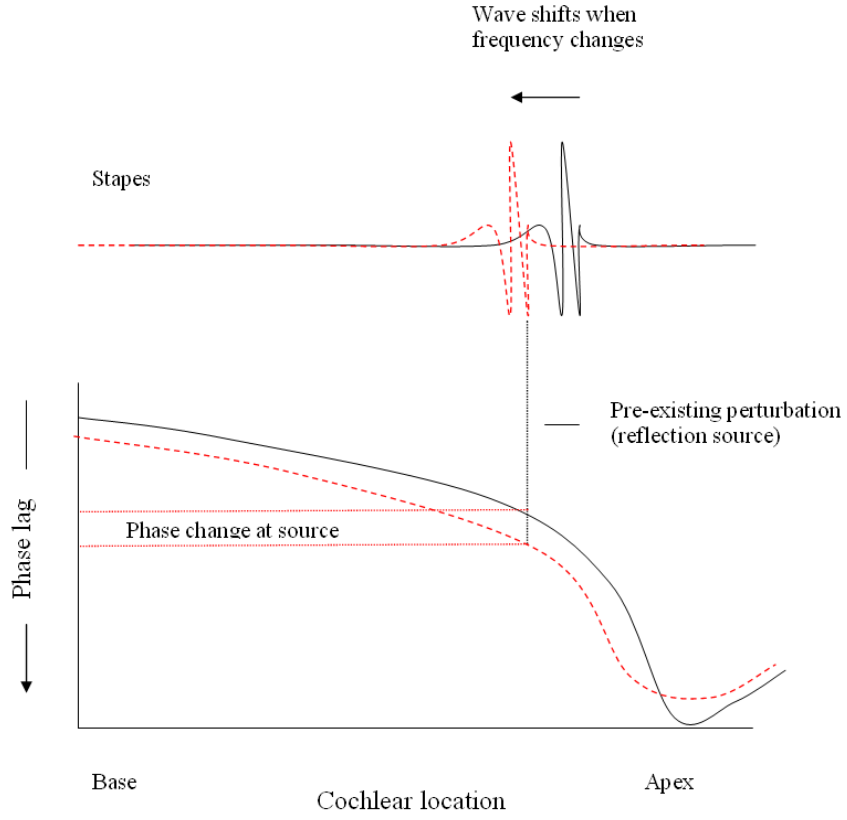

Figure 1.4 Similar diagram as Figure. 1.1 demonstrating a reflection source. As a consequence of pre-existing mechanical perturbations that are stationary, the phase of the TW reaching the perturbation, and subsequently the phase of the scattered wave, changes significantly with stimulus frequency. The above figure shows one imperfection, in reality there are many more. In the example above the red stimulus is higher in frequency than the black, so has greater amplitude. Source: Shera, 2004, page 5.

Many of these scattered wavelets combine out of phase and may cancel out. An anologue of Bragg's law from x-ray crystallography enables scattered wavelets to accumulate creating a large reflected wave. The region of reflection moves along the cochlear partition as frequency is changed (Shera and Guinan, 1998). This is clearly exemplified in Figure. 1.4. Non-linear distortion and linear coherent reflection both contribute to all evoked OAEs as they combine in the ear canal (Kalluri and Shera, 2001; Shera et al., 2004; Shaffer, 2003). This is demonstrated in Figure. 1.5 for DPOAEs.

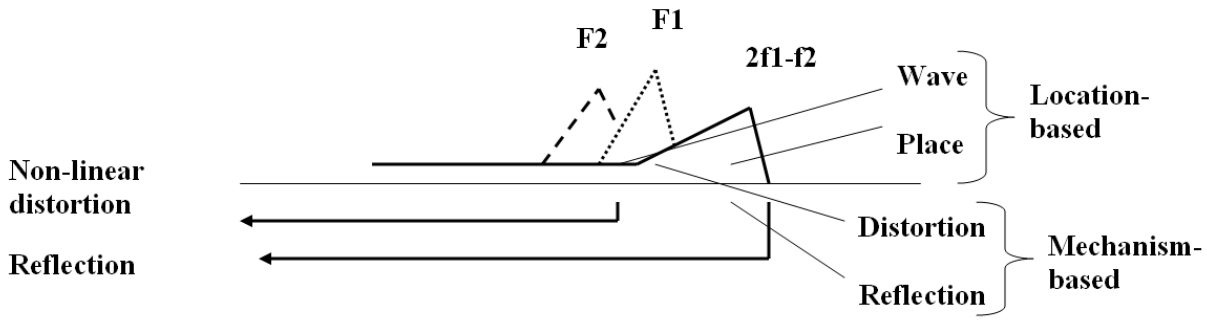

Figure 1.5 The origin of non-linear distortion resulting from the region of overlap of the two stimulus waves. The two waves interfere and the recordings made arise from these two separate generation mechanisms, as they mix in the ear canal. Source: Shaffer et al., 2003, page 369.

In the next section the experimental methods concerning how the two components are separated are discussed. The two main approaches are by studying phase gradients and the introduction of a suppressor tone.

1.4.2 Phase gradients

The phase pattern of an OAE can give information concerning the underlying mechanisms of their creation. The phase of a TW moving through a specific place on the BM has a recognisable gradient as the frequency of the stimulus is varied (Robinette and Glattke, 2007). The phase gradient of a reflecting point will alter as it moves back to the middle ear. As the stimulus frequency is lowered, the TW peak shifts toward the apex keeping approximately an equal number of waves within its TW envelope (Robinette and Glattke, 2007, page 31). The TW would however have less full cycles before reaching the reflective place.
For the distortion component phase will alter little as a consequence of stimulus frequency change. This is because the number and placing of waves varies slowly with frequency. Essentially it is related to the bandwidth of tuning, which is broader at higher frequencies resulting in less delay at higher frequencies.

The place-fixed characteristic will have a steeper phase than the wave-fixed characteristic (Robinette and Glattke, 2007; Knight and Kemp, 2000).

Knight and Kemp (2000) investigated the place and wave- fixed dichotomy by using a range of 2f1− f2 and 2f2− f1 DP stimulus frequency sweep data, where the 2f2− f1 DP is more basal than the 2f1− f2 DP (as the frequencies are higher). Knight and Kemp (2000) used a time window separation technique. The authors examined the influence of stimulus frequency by various methods including by sweeping f1, f2 and by sweeping both frequencies simultaneously in order to ensure a constant frequency ratio. Knight and Kemp (2000) displayed their findings in matrices visually demonstrating how the two different DPs are related and how DP phase and magnitude are influenced by frequency. In each data chart the 2f1− f2 data were located in the upper portion, and the 2f2− 1 DP data were located in the lower portion. Knight and Kemp (2000) discovered that there is a systematic change in the proportion of wave and place-fixed emissions. In the 2f1− f2 portion a wide stimulus frequency ratio results in wave-fixed emissions, whilst all other DPs are place-fixed. A transition occurs in this portion at f2/f1 = 1.1. This provided evidence that the mechanisms underlying the origin of 2f2− f1 and 2f1− f2 at lower frequencies ratios are fundamentally the same, but at greater frequency ratios there is an alternate source for the 2f1− f2 DP. Knight and Kemp (2000) suggest that these findings support the model that for wave-fixed emissions DP energy is largely created in the f2 region and is emitted directly. For other DPs even though the DP is generated due to the non-linearity within the f2 envelope, the DP is emitted by a combination of non-linearity and a reflection mechanism.

The dominance of the direct emission (wave-fixed) was also emphasised by a separate investigation conducted by Knight and Kemp (2001) using a phase gradient dependent post-processing method. Knight and Kemp (2001) separated wave and place-fixed components of DPOAEs. By utilising an inverse Fourier transform of a DP sweep with a fixed frequency ratio a quasi-time domain pattern with two separate peaks can be created, the magnitudes of which are dependent on the frequency ratio of the sweep. The distinct peaks are a consequence of the different phase gradients. Knight and Kemp (2001) windowed the low and high latency components in the pseudo-time domain and then converted this back to the frequency domain independently. Interference between the two emission components results in overlapping of measurements but they have different level, phase and suppression characteristics, which can be seen on frequency domain maps (Knight and Kemp,

2001). Low-latency components are only emitted strongly with f2/f1 between 1.1 and 1.3. The high-latency component is present more widely in the lower f2/f1 ratios. For all but the close primary condition the lower sideband DPOAE (i.e. 2f1− f2) was dominated by direct emission from the region of f1 and f2 wave interaction (wave-fixed emission) (Knight and Kemp, 2001).

In summary there are different terms used to describe the components of the DPOAEs. These differences arise because of the different ways of classifying them. The distortion and reflection component are classified according to the mechanism of generation, the wave-fixed and place-fixed the location. Throughout this document the two different classification terms will be used interchangeably.

1.4.3 Fine Structure

The level dependent shift of DPOAE fine structure can be demonstrated experimentally on participants (He and Schmiedt, 1997; Mauermann, 1999), and by computer models (Sun et al., 1994 [a+b]; Mauermann, 1999). Both Mauermann et al. (1999) and He and Schmiedt (1997) measured the fine structure of the 2f1-f2 acoustic distortion product (ADP) in the human ear canal with different primary levels. Sun et al. (1994[a]) created a computer model to replicate the behaviour of ADP fine structure. The dependency of ADP fine structure patterns on the frequency ratio of f2/f1 was studied in the participants under two experimental conditions, by altering f1 or f2 (fixing f2 and f1 respectively). Mauermann et al. (1999) and He and Schmiedt (1997) made further investigation by changing both primaries at a fixed ratio and observing different order DPOAEs. As L1 was fixed and L2 was varied an upward frequency shift was observed in the ADP fine structure as L2 increased. As L2 was fixed and L1 varied, downward frequency shifts were observed. These opposite frequency shifts are the same as those predicted by the model developed by Sun et al. (1994[a]).

The investigations of ADP in the ear showed that fluctuations in DPOAE level up to 20 dB could be measured. In contrast, the results from a fixed fDP paradigm indicate no fine structure, but a dependence of DP level on the f2/f1 ratio, with a maximum 2f1− f2 with a ratio approximating 1.2 (Mauermann et al., 1999). He and Schmiedt

(1997) report a similar ratio, with the largest rate of shift associated with a ratio of 1.11.

In a further investigation into this topic Sun et al. (1994[b]) increased the mean damping factor non-linearly with input level to replicate the frequency shift of the peak of the TW observed in experimental data. The resulting model mimics an ADP that is compatible with data from participants wherein the ADP fine structure does not saturate with level. The input/output functions (I/O) of the simulated ADP emissions were also investigated. It was revealed that the functions depend on the pattern of ADP fine structure and the I/O frequency. It must be noted that there is a fine structure present in SFOAE (and hearing thresholds) where only a single frequency is present (Talmadge et al., 2000; Mauermann et al., 2004).

These experimental results and those from computer simulations of DPOAE provide evidence for a two-source model of the cochlea. The first source being an initial non-linear interaction of primaries near the f2 place, and the second reflection from a re-emission site at the characteristic place of the DP frequency.

1.4.4 Mixing and un-mixing

If this theory of the mechanism underlying the emission of DPOAE is accurate, that DPOAE are the result of a mixing of the two components distortion and reflection, then it should be possible to un-mix DPOAEs into the separate components. The frequency dependence of their phases will be consistent with the mechanism underlying their origin. The reflection source component of the total DPOAE should closely match the reflection source emission recorded at the same frequency under similar conditions (Kalluri and Shera, 2001).

1.4.5 Evidence through experimentation

An experimental approach that has often been adopted to utilise the spatial separation of the two 2f1− f2 DPOAE components is selective suppression by the introduction of a third tone, near in frequency to the DPOAE (Talmadge, 1999; Mauermann et al.,

1999; Gaskill and Brown, 1996; Kummer et al., 1995; Kalluri and Shera, 2001). Pioneering experiments using this technique were carried out by Kemp and Brown (1983, in Kalluri and Shera, 2001). The suppressor tone reduced the amplitude of the wavelets incident upon and/or scattered back from the reflection region. A suppressor tone with a frequency closer to the total DPOAE should have a greater impact on the amplitude of the reflection site component than the non-linear component (Talmadge et al., 1999). According to theory based models as the suppressor tone level increases, initially there will be no evident effect, but will eventually result in the decline of the reflection component. As the third tone rises in level at some point it suppresses both components and consequently the total recorded level of the DPOAE (Talmadge et al., 1999) (Figure. 1.6). Is this what is found in practice?

Talmadge et al. (1999) investigated this paradigm in four participants with an age range of 20-54 years, the participants were selected after extensive screening procedures, including multi-frequency tympanometry, audiometry, audiological history, and the evaluation of spontaneous, transient evoked and DP otoacoustic emissions. Utilising continuous primaries the third tone induced two effects on the level and phase of the fine structure.

The first observation is that when apical reflection is initially greater than the overlap region increasing the suppressor level initially results in the reflection becoming approximately equal to the overlap region non-linear distortion component and subsequently deepens the amplitude fine structure. When the distortion component is equal in amplitude to the reflection component there is enhancement due to constructive interference at maxima and reductions due to destructive interference in the minima; this process leads to the enhancement of the fine structure (Talmadge et al., 1999). The phase behaviour remains ramp like; the phase shifts by 360^{o} over a small frequency range, giving a ramp like pattern when plotting phase against frequency in constant f2/f1 sweeps. Once the suppressor level is high enough, the reflection component becomes less, and the amplitude fine structure begins to decrease until it disappears altogether. High enough suppressor levels reduce both reflection site and overlaps, and the total DPOAE decreases (Talmadge et al., 1999).

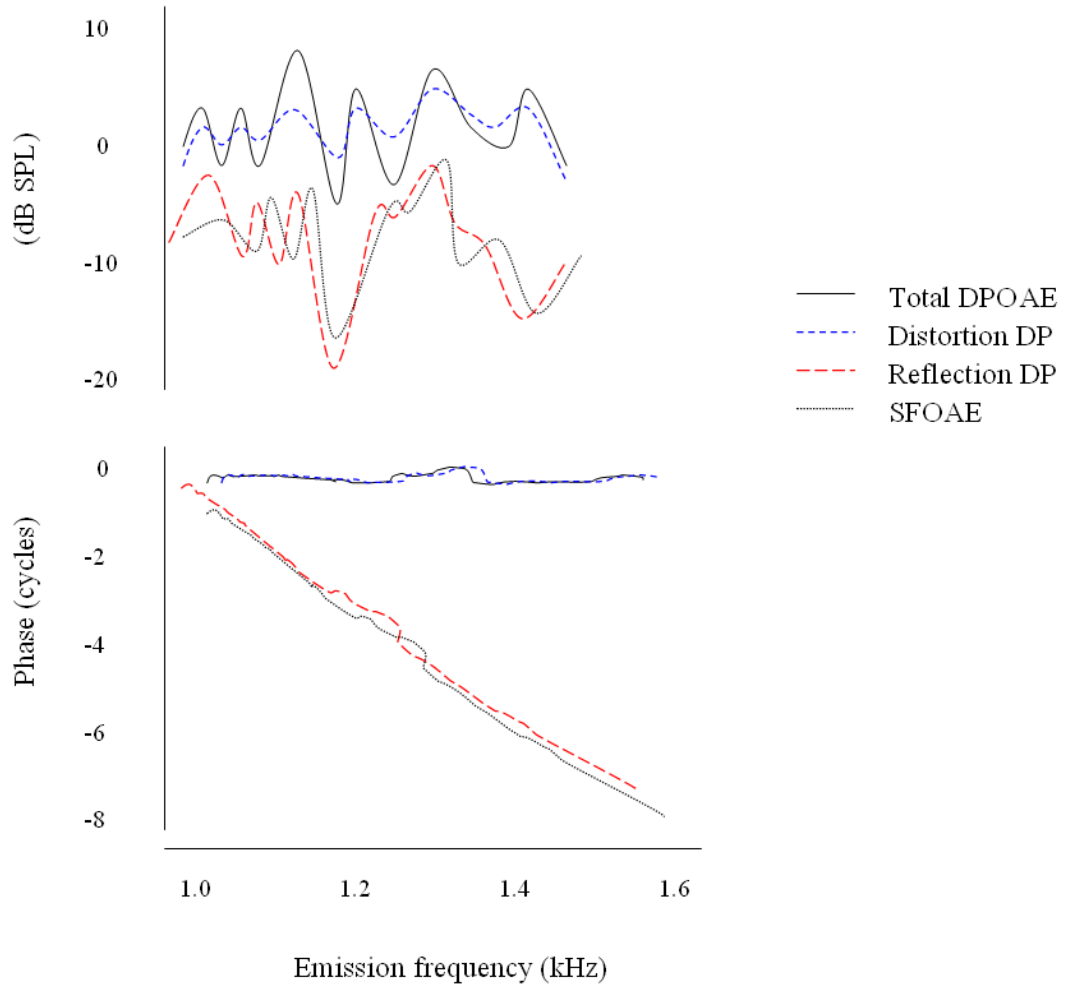

Figure 1.6 The amplitude (top) and phase (bottom) of the total 2f1– f2 DPOAE (solid line) and separately the non-linear distortion source (dashed line) and reflection source (punctuated line) found using third tone suppression based un-mixing. DPOAE stimulus parameters L1, L2 = 60, 45 dB SPL respectively, f2/f1= 1.2. The grey lines exemplify the SFOAE recorded in the same participant at a probe level of 40 dB SPL. The SFOAE was measured in the presence of a third tone with the same characteristics as the f1 primary used to evoke the DPOAE. Source: Shera, 2004, page 6.

1.4.6 The third tone and fine structure predictability

Further evidence for this occurring for the 2f1− f2 DP is presented by Kummer et al. (1995). Using low-level primary tones the authors report particular sensitivity to suppressor tones near Fdp. Below thresholds above which suppression generally occurred, the DPOAE was largely suppressed, forming low-level regions of

suppression-growth functions. At suppressor levels above normal thresholds, steeper suppression developed. Kummer et al. (1995) suggest the two regions of the suppression growth functions are due to interference at different cochlear sites. Gaskill and Brown (1996) demonstrated similar findings concluding that the measured DPs in the ear canal originate from the DP frequency region, along with those from the primary frequency region. By introducing the third tone similar in frequency to the DPOAE, a change can be induced in the patterns of amplitude, phase, and group delay of the DP (Talmadge et al., 1999). The fact that it is possible to alter the correlation between group delay and fine structure pattern with the introduction of the third tone suppressing the DP component is further evidence supporting the two-source theory.

Konrad-Martin (2001) recorded the 2f1− f2 DPOAE in the ear canals of nine normally hearing participants, utilising a fixed f2 paradigm, and varying f1. The frequency of f2 was fixed at either 2 or 4 kHz, and absolute and relative primary levels altered. In one of two experimental conditions a third tone f3 was introduced to act as a suppressor situated 15.6 Hz lower than 2f1− f2. An inverse fast Fourier transform (IFFT) was used to change the recordings from the complex (sweep) frequency domain into an equivalent time domain. Similar findings were observed to those of Talmadge et al. (1999). A suppressor tone situated below the 2f1− f2 frequency resulted in declines, or abolished all together components in the time envelope with longer latencies. The lower latency components were unchanged. This implies that the eliminated components were the result of secondary DPOAE source activity, created close to the DP place (by reflection).

The use of a suppressor tone secondly reduced microstructure in DPOAE level and phase responses. Kalluri and Shera (2001) also used the Fourier analysis technique, applying it to frequency domain measurements, and suggested that the components have different latencies. A shorter latency is exhibited by the distortion component and a longer latency corresponds to the reflection component. Heitmann et al. (1998, in Mauermann et al., 1999) also showed that fine structure disappears when the DPOAE is measured with a third tone close to the DP frequency as a suppressor. Similar findings are demonstrated in Gaskill and Brown (1996), Dreisbach and Siegel

(1999) and Kummer et al. (1995). The latter authors however report that in some instances a suppressor close to 2f1− f2 results in more suppression than close to f2.

The position of the suppressor relative to the DP has an effect on the extent of suppression on the DP, as reported by Gorga et al. (2002). Gorga et al. (2002) report results for a suppressor fixed at either 2.1 or 4.2 kHz, set to levels between 20-80 dB SPL. Suppressor level was fixed and f2 varied and compared to a control condition in which no suppressor was present. The decrement plots revealed the largest suppression when the suppressor frequency (f3) was approximately equal to f2. Steeper slopes of DPOAE decrement versus suppressor level function were obtained when f2>f3 relative to f2<f3.

1.4.7 Pulsed and continuous tones

Talmadge et al. (1999) further tested the model by observing the temporal behaviour of a DPOAE when one of the primaries is pulsed and the other is kept on continuously. The f2 primary tone was pulsed on and off (pulsed for 100 ms every 250 ms) whilst the f1 primary tone was at a continuous level. Under circumstances in which the overlap region component is expected to be dominant from fixed ratio measurements, an interference notch is observed in the DPOAE amplitude shortly after-turn off of the f2 primary. When the DP tonotopic place is expected to be dominant from fixed ratio measurements, an interference notch is observed in the DPOAE amplitude shortly after turn-on of the f2 primary (Talmadge et al., 1999). These notches are a consequence of destructive interference between the two components and occurs when the two components are similar in level.

1.4.8 A few criticisms

Often in DPOAE investigations the participant numbers are very low. Knight and Kemp (2001) for example only used two participants. These low participant numbers compromise the accuracy of interpretation. Issues surrounding the introduction of a suppressor tone need to be discussed. The suppressor tone may also change the response in other ways, such as by suppressing the distortion source or leading to the

creation of more distortion sources. Incomplete un-mixing may also occur; there is always a trade-off scenario as the third tone is either too weak or too strong. This results in either residual components still being present or interference. It would also be interesting to discover if the techniques give similar results if different f2/f1 ratios were used, and the influence of different stimulus levels. It is essential that investigations of DPOAEs are carried out in conditions of low background noise.

Knight and Kemp (2001) report that the dominating component of the elicited DPOAE is dependent on the parameters of the stimulus. It can be difficult to make comparisons between investigations of this type if different stimuli are used, such as the differences between Knight and Kemp (2001) and Tubis et al. (2000) (in Knight and Kemp, 2001). The Knight and Kemp (2001) model did not incorporate reflections back off the stapes. These models are also based on theoretical assumptions of cochlear mechanics, such as the emission being sourced from a point as opposed to over a region; cochlear characteristics such as hydrodynamics and degree of amplification (Shera et al., 2000). Shera et al. (2000) conducted their investigation on albino guinea pigs- it is difficult to know how this relates to other species including humans. In reality it can be difficult to interpret emissions due to the interference between different emission types.

The condition of the cochlea and middle ear function may have an impact on DPOAE measures, and cause individual variation from session to session (Shera and Guinan, 1999). Minor differences in the place where the probe is situated, and how the probe is assembled can lead to large measurement alterations. SOAEs can also influence results.

Talmadge et al. (1999) report how utilising group delays via IFFT technique is not a direct measure and can be complicated to interpret theoretically. DP-fine structure amplitude can even vary through the course of a single session. In Talmadge et al. (1999) issues also arise with the interpretation of the results. Fine structure can still be seen even if only one source is present; some authors seem to ignore this fact. Gaskill and Brown (1990) used a larger number of participants, 34, including both genders 19 female and 15 male, and with an age range 15-50 years. However, because of the possible risks to the participants, tympanometric measurements were

not made except in the ear canal of the two authors. The reasons underlying this were not specified. Variation in middle ear pressure can affect results by altering loading on the cochlea.

1.5. Clinical utility

1.5.1 The principles of TEOAE and DPOAE

There are two main types of OAEs, spontaneous and evoked. Evoked emissions can be sub-classified further as a result of the evoking stimulus parameters: Transient evoked otoacoustic emissions (TEOAEs), stimulus frequency otoacoustic emissions (SFOAEs) and distortion product otoacoustic emissions (DPOAEs) (Lonsbury-Martin and Martin, 1990). The use of OAEs in a clinical setting was first proposed by Kemp (1978). OAEs are recognised as being a non-invasive, objective measure of cochlear function. They are a very repeatable measure and are easy and quick to detect (Lonsbury-Martin and Martin, 1990).

There are two main methods used in clinical practice at present: 1) click or transient evoked OAE and 2) the DPOAE method. OAE measurements are made with the use of an ear canal probe that is placed down the external auditory meatus. This reduces background noise and ensures that more of the OAE is measured. A series of click stimuli are then transmitted into the ear at approximately 84 dB SPL peak equivalent (p.e) level, to produce a TEOAE in the non-pathological ear (Kemp, 2002; Robinette and Glattke, 2007). The response can be divided by frequency making it easier to interpret results from the various parts of the cochlea (Kemp, 2002). Results are best for analysing between 1 and 4 kHz. Measurements of OAEs are a valuable tool in clinical audiology, as in most ears with conductive or cochlear pathology they are not emitted (Robinette and Glattke, 2007). This is why TEOAE detection forms a vital part of newborn hearing screening programmes.

The other technique for measuring OAEs is to use DPOAEs and they are also utilised in a clinical capacity. These emissions are inter-modulation distortion tones originating in the cochlea as a result of stimulation by a close pair of stimuli

(Robinette and Glattke, 2007). Recording DPOAEs involves varying the frequency of the two stimulus tones. The probe contains two small loud speakers (f1 and f2), which are inserted into the ear canal. The probe must also contain a small microphone (Lonsbury-Martin and Martin in Robinette and Glattke, 2007, page 108). A method for recording DPOAEs can be seen in Figure. 1.7. A DPOAE is assessed to be present when the level of the DPOAE is greater by some amount than the average noise level (Lonsbury-Martin and Martin in Robinette and Glattke, 2007, page 111).

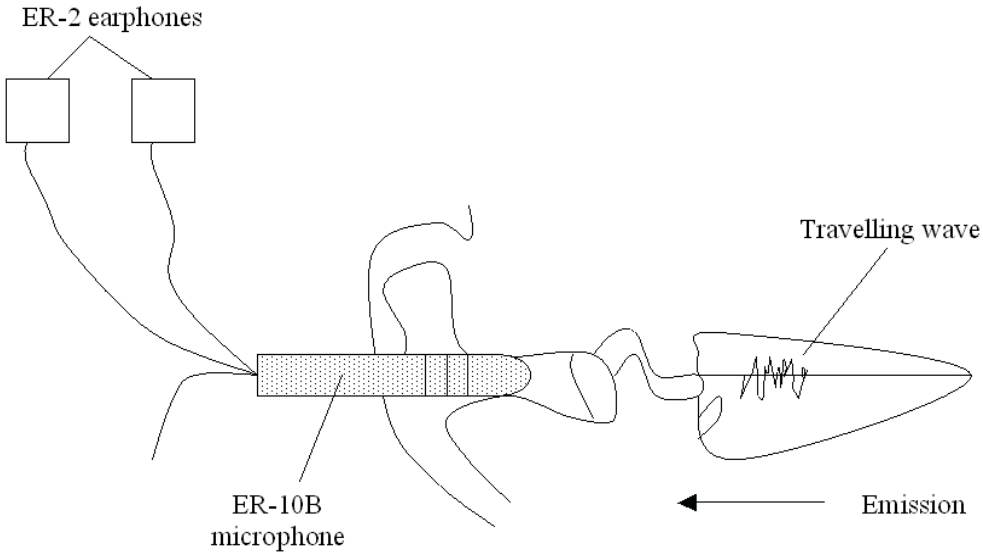

Figure 1.7 A simple technique that can be implemented to record DPOAEs in the ear canal. Two earphones (ER-2) produce the stimuli, and the recording device is a small microphone (ER-10B). Source: Lonsbury-Martin and Martin, 1990.

The elicitation of evoked OAE emissions is highly dependent on stimulus parameters (Robinette and Glattke, 2007; Miller and Marshall, 2001; Kemp et al., 1990; Boege and Janssen, 2002).

Two such parameters are the levels of the primary tones (L1 and L2) and the level separation of the primary tones (L1-L2) (Robinette and Glattke, 2007, page 124; Boege and Janssen, 2002). Equal primary tone responses at the f2 place are considered to be the optimal conditions for eliciting DPOAEs. As primary tone level is decreased, largest DPOAEs are exhibited when using a rising primary tone separation L1-L2. This is due to properties of the BM (Boege and Janssen, 2002). The linear equation L1 = 0.4*L2 + 39 dB expresses the primary tone levels expected to give the largest amplitude of DPs using a frequency ratio of 1.22.

The frequency ratio of f1 and f2 also has a determining role in how much variation there is in DPOAE level as hearing threshold varies.

1.5.2 The DP-gram and I/O functions

A DPOAE audiogram (DP-gram) can be used to obtain objective information of cochlear function. A DP-gram plots emission level relative to frequency. To create a DP-gram data are collected across a variety of frequencies (0.1 octave intervals) for three primary-tone levels; 65, 75, and 85 dB SPL, with L1 = L2 and f2/f1 = 1.22 (Lonsbury-Martin and Martin, 1990). In most current systems, DPOAE amplitude is deemed to be the level of DPOAE-frequency bin that includes the DPOAE and the background noise. This bin is studied alongside adjacent bins in which no DPOAE measure was made. A DPOAE is regarded as present when the bin containing the DPOAE measurement is greater by a certain degree relative to the other bins (Robinette and Glattke, 2007, page 111). In the non-pathological ear the mean DPOAE level is estimated to be 5 dB SPL, with a standard deviation of 5 dB between 1 and 7 kHz.

Along with the DP-gram, information can be portrayed as an input/output function (I/O). In this form the DPOAE amplitude is described in relation to the level of the primary tones, for rising stimulus levels (Robinette and Glattke, 2007, page 111). An example can be seen in Figure. 1.8. These I/O functions display OHC responses to both threshold and supra-threshold stimuli. Results for DP-grams and I/O functions can be compared between normal hearing ears and impaired ears (Lonsbury-Martin and Martin, 1990).

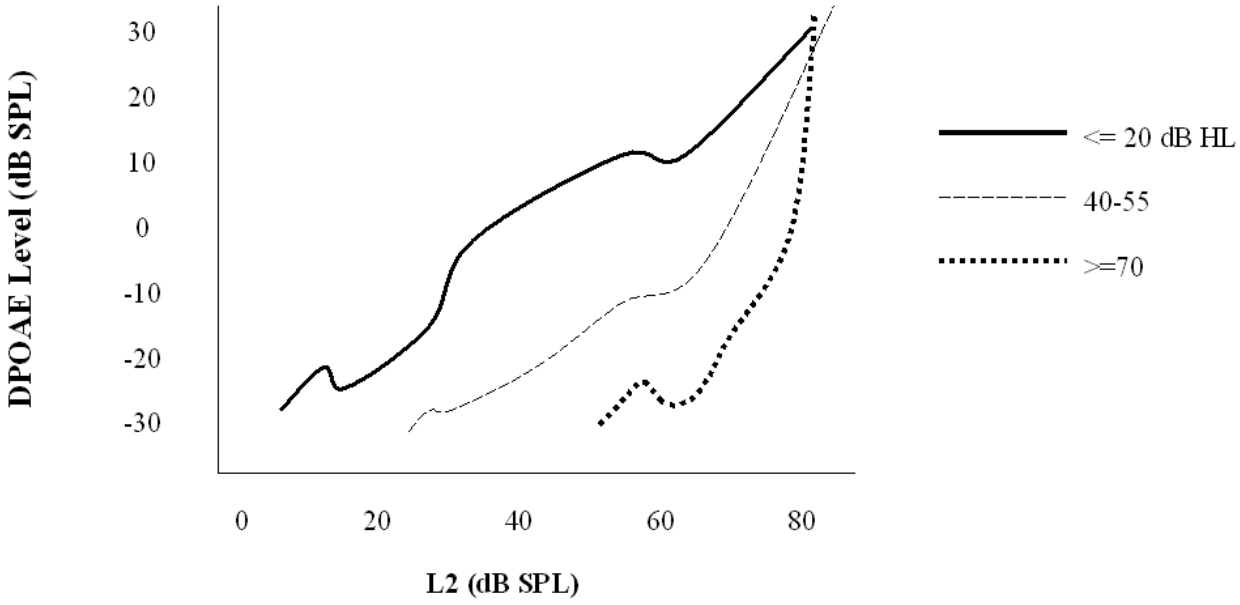

Figure 1.8 DPOAE I/O functions at f2 frequency = 1 kHz in participants with normal hearing, and various levels of hearing impairment. Source: Dorn et al., 2001.

1.6 Current issues

1.6.1 Issues surrounding DPOAEs and threshold estimation

Except for in research conditions it can difficult to fit the otoacoustic probe perfectly, as a result of variations in meatal shapes, and a restricted time for carrying out the procedure (Kemp et al., 1990; Boege and Janssen, 2002). Variations in middle ear condition, such as the presence of fluid, can also create pressure imbalances that can lead to a decline in the emission energy below 2 kHz, rising above 3 kHz (Kemp et al., 1990; Boege and Janssen, 2002). The presence of spontaneous otoacoustic emissions potentially enhances the DPOAE amplitude (Osterhammel et al., 1996; Kimberley et al., 1994). Standing waves forming in the outer ear could also affect calibration when using microphones at frequencies above approximately 1.5 kHz (Siegel et al., 2005). These variations mean that there is a very large degree of inter-subject variability creating low repeatability of DPOAE measurements, even in ears with normal hearing (Suckfull et al., 1996; Kummer et al., 1998, Figure. 1.9).

Robinette and Glattke (2007) explain how occasionally damage to the cochlea results in more behavioural or evoked potential threshold elevation as opposed to DPOAE declines. Investigations into DPOAEs evoked by high intensity stimuli (above 65 to 70 dB SPL) do not show the mechanics of the cochlear amplifier, or that of the OHCs, but there is a gap in our knowledge regarding how much this relates with humans. Human ears with normal thresholds can also exhibit reduced or absent DPOAEs over certain frequency ranges (Robinette and Glattke, 2007), for reasons that are unclear.

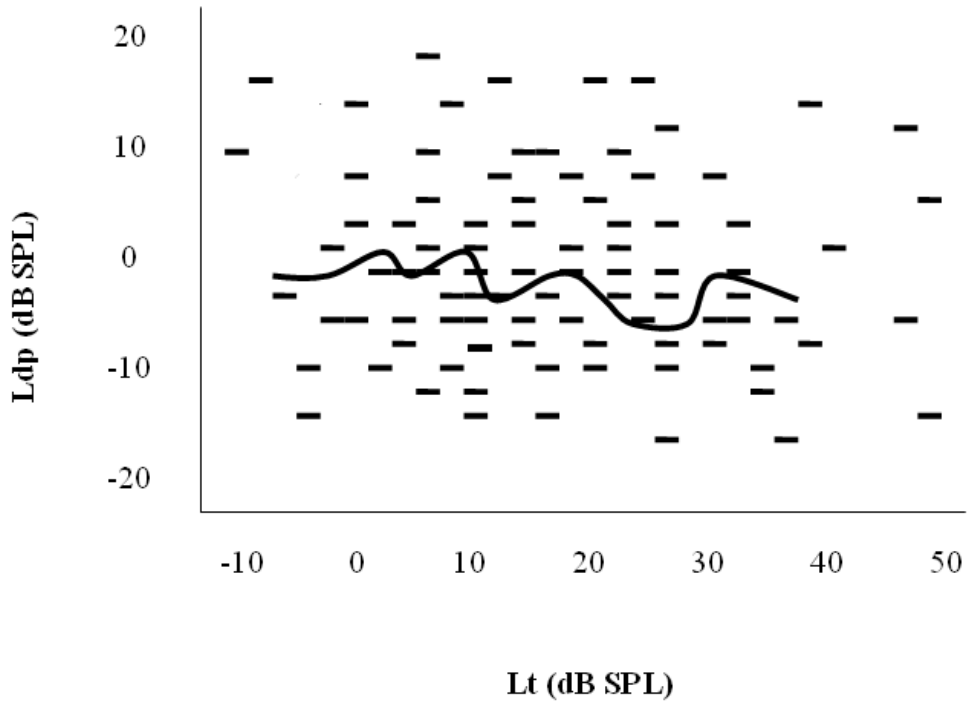

Figure 1.9 Complete DPOAE data from 20 normal hearing ears, plotted against threshold level L. DP level Ldp, for L2 = 60 dB SPL (SNR > 6 dB). Source: Kummer et al., 1998.

1.6.2 A few unknowns and OAE group delay

There are still a large number of unknowns surrounding DPOAEs that inhibit both the understanding of the mechanisms occurring within the ear, and how they are used in the clinical environment. These issues largely surround the mechanisms of generation of DPOAEs. The most common theory that the cochlea makes sound created by

backward TWs has been called into question (Robinette and Glattke, 2007, page 124). The likelihood of compressive waves moving through the cochlear fluids being the route for OAEs to reach the middle ear, as opposed to a backward BM TW, is currently being studied.

Many authors have investigated group delay and the site of DPOAE generation (Ren, 2004; Ruggero, 2004; Siegel et al., 2005; Ren et al., 2006). Ren et al. (2006) utilised a technique in Mongolian gerbils whereby the auditory bulla was exposed through a ventral lateral surgical method and made measurements of BM motion using a laser interferometer. A sensitive microphone recorded the sound pressure in the external ear canal. This analysis revealed that cochlear round trip delay is decreased corresponding to intensity indicating that the emission location moves toward the base with intensity. The decrease in delay is a result of a wider bandwidth of tuning at higher intensities. The group delay was less than or equal to the forward wave. The group delay at the stapes was also equal to or smaller than the forward group delay. These findings are similar to those of Ren (2004). Ren (2004) using a similar technique found that the slope of 2f1− f2 corresponds with movement of the BM vibration being largely dictated by a forward TW. The stapes was also discovered to vibrate earlier than the BM. This is consistent with a reflection generation mechanism, as described earlier. The difference between the timing of the stapes vibration and the BM vibration can be seen in Figure. 1.10. The discovery that the BM vibration located at the OAE frequency is determined by a forward TW and that the stapes vibrates before the BM is evidence contradicting the backward TW theory.

When interpreting these investigations it is important to note that Mongolian gerbils are unlike humans, as they do not have a reflection component to their DPOAEs. Also less sharp filtering at the same place may lead to shorter delays. This highlights the fallacy of equating distance and time when the TW is not at a constant speed.

Ruggero (2004) identified results that are applicable to the hypothesis that either OAEs propagate via acoustic compression waves in the cochlear fluids or as a result of backward TWs, but was unable to separate the two.
Siegel et al. (2005) expanded upon the work of Ren (2004) by examining the entire length of the chinchilla cochlea as well as areas of the guinea pig and cat cochlea.

Siegel et al. (2005) found in chinchilla that SFOAE group delays were similar to or shorter than BM group delays for frequencies >4 kHz and <4 kHz, respectively. These short delays are evidence against the theory of coherent reflection filtering.

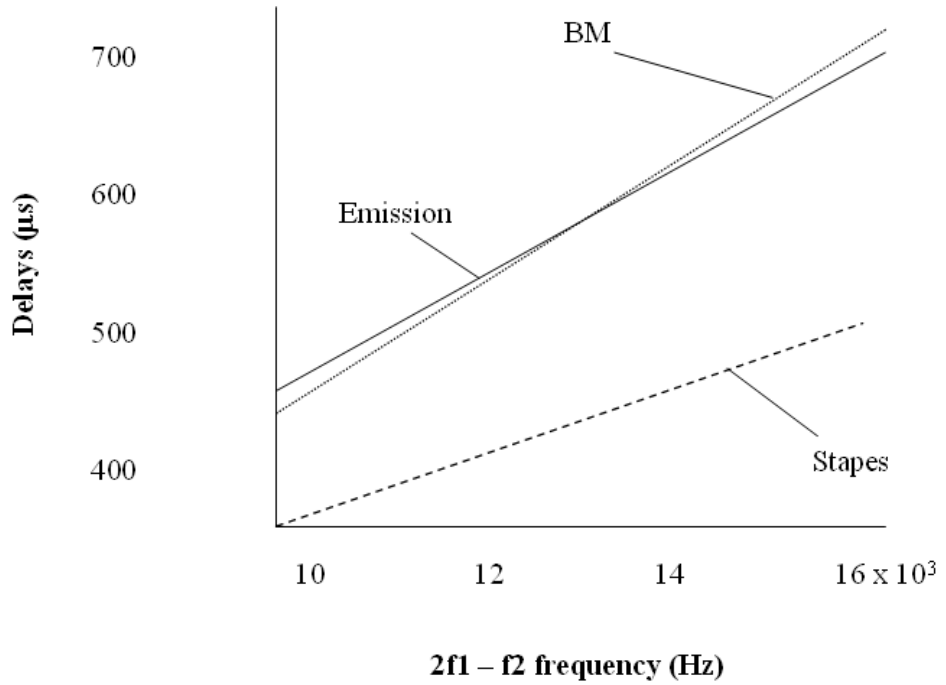

Figure 1.10 Frequency response of the BM, stapes and ear canal sound pressure to fixed f2 (17 kHz) and frequency altered f1. The stapes vibrates 50 μs before the BM. Source: Ren, 2004.

Further evidence for the compression wave idea was indirectly presented by van Dijk and Manley (2001) as they identified DP in the tree frog *Hyla cinerea* despite the fact that their hearing organs do not sit on the BM. This is in direct contrast to the findings of Baker et al. (1989) who did not find DPOAE in three species of frog, *Rana temporaria, R. pipiens,* and *R. esculenta* (Dijk and Manley, 2001). Robles et al. (1997) discovered that in situations where the stimulus tones had large gaps between frequencies, the responses to the primaries were tiny and increased approximately linearly, in contrast to 2f1− f2 responses that were bigger and increased more compressively. Robles et al. (1997) suggest that this means that DPs do not originate at the measurement site but from a more basal location and move toward the 2f1− f2 site.

1.6.3 The 2f2− f1 cubic distortion product

There is a limited amount of literature concerning the origin of the 2f2− f1 emission. Some authors do indicate that the generation site is located basal to the DP frequency place along the BM (Wilson and Lutman, 2006; Erminy et al., 1998). Martin et al. (1987 in Wable et al., 1996) investigated the 2f2− f1 DP in the rabbit ear, and contrasted it with the 2f1− f2 DP. The 2f2− f1 DP was found to originate from a region more basal to the relative frequency places. Martin et al. (1998) demonstrated that in normal hearing humans the 2f2− f1 DP is generated basal to the primary-tone place on the BM. This implies that the 2f2− f1 DP could reveal different information concerning cochlear function than the 2f1− f2 DP. Wable et al. (1996) used latency as a means of gathering information concerning the generation sites of the 2f1− f2 and 2f2− f1 DP in humans. It was revealed that amplitudes were lower (mean difference of 10.5 ± 4.2 dB at 70 dB and 10.2 ± 4.6 dB at 55 dB) and latencies shorter for 2f2− f1 in comparison to 2f1− f2. Moulin and Kemp (1996) also exemplified that for lower sideband DPOAEs an f2 sweep resulted in greater time delay than the f1 sweep, in contrast to the 2f2− f1 DP where no difference was observed. Moulin and Kemp (1996) suggest that this implies the DPs do not originate from the same aspect of the TW. Further research is needed as evidence of these investigations indicates a potentially different generation process for the 2f2− f1.

Erminy et al. (1998) also concluded that there were large variations between the behaviour of 2f1− f2 and 2f2− f1 DP, potentially as a result of different generation mechanisms. Differences included at high frequencies (i.e. f2 > 4 kHz) the prevalence of 2f2− f1 declined, whereas by contrast the 2f1− f2 remained the same. Thus the 2f2− f1 DP appears to have greater dependence on frequency. Wable et al. (1996) suggest that a comparison of both DPOAEs would be a valuable tool in assessing cochlear function.

Martin et al. (1997) explain how the 2f1− f2 amplitudes remain relatively constant whilst the 2f2− f1 levels showed great variation. As both emissions were generated by the same set of primaries, this indicates a difference in some underlying generation

mechanism. This is further implied by the differences in amplitude between the two emissions.

Knight and Kemp (2001) discovered in one of their two participants, the 2f2− f1 DP contained two components. When the frequency is varied one component (wave-fixed) exhibited a constant phase, and the other (place-fixed) exhibited a sloping phase. Knight and Kemp (2001) suggest that for the 2f1− f2 wave-fixed emission the DP originates in the f2 region and is emitted directly. This is problematic as the TW cannot propagate at the DP frequency at the f2 place. All other DPOAEs are described by Knight and Kemp (2000) as place-fixed, and the DP is not directly emitted but moves apically, where it is re-emitted basally as a consequence of a reflection mechanism. Knight and Kemp (2001) document that in one of their two participants (RN) both a wave-fixed and place-fixed component in the 2f2− f1 DP were present, but could not define it as being a normal characteristic as it was only located above the noise in a single participant. Knight and Kemp (2001) report that the origins are potentially in the region of the DP frequency place in the cochlea.

Wilson and Lutman (2006) used an experimental design to identify the wave and place-fixed components of both the 2f1− f2 and the 2f2− f1. The investigation included 20 non-pathological adult ears. The investigators used four frequency ratios f2/f1 = 1.05, 1.10, 1.22, and 1.32. Fixed frequency sweeps were collected and plotted as a function of f2. Wilson and Lutman (2006) found evidence supporting the existence of a wave and place-fixed component of the 2f1− f2. They also discovered that in the majority (18) of the participants the wave and place-fixed components were present for 2f2− f1. The 2f1− f2 emission had a wave-fixed component that had largest magnitude at f2/f1 = 1.22, and the place-fixed component remained unchanged. The 2f2− f1 emission had a greater place-fixed component and a smaller wave-fixed component, both of which do not have a strong dependence on frequency ratio (Wilson and Lutman, 2006). Wilson and Lutman (2006) proposed a mechanism of generation of the 2f2− f1 DP, which can be seen in Figure 1.11. The authors suggest that the DP wave may be created at any location basal to the DP frequency place. Waves of the primary frequencies f1 and f2 travelling past the 2f2− f1 DP place are basal to the characteristic frequency so subsequently are not slowed by the mechanics of the cochlea. It is suggested that non-linearity at the 2f2− f1 DP place

results in energy being emitted basally through a reverse TW or a through the cochlear fluids. As neither of the primaries has reached their characteristic place, this may explain why this component is so small for the 2f2− f1 DP (Wilson and Lutman, 2006). Wilson and Lutman (2006) state that potentially the reflection and distortion emissions are in operation at the DP frequency place, or basal to it.

Sharp (2007) used similar parameters as Wilson and Lutman (2006) but used a suppression method to investigate 2f2− f1 and 2f1− f2. Sharp (2007) explains how unlike the time window separation technique the suppression method relies on the two components being physically remote. Sharp (2007) confirmed that both wave and place- fixed components are evident in the 2f2− f1 DP.

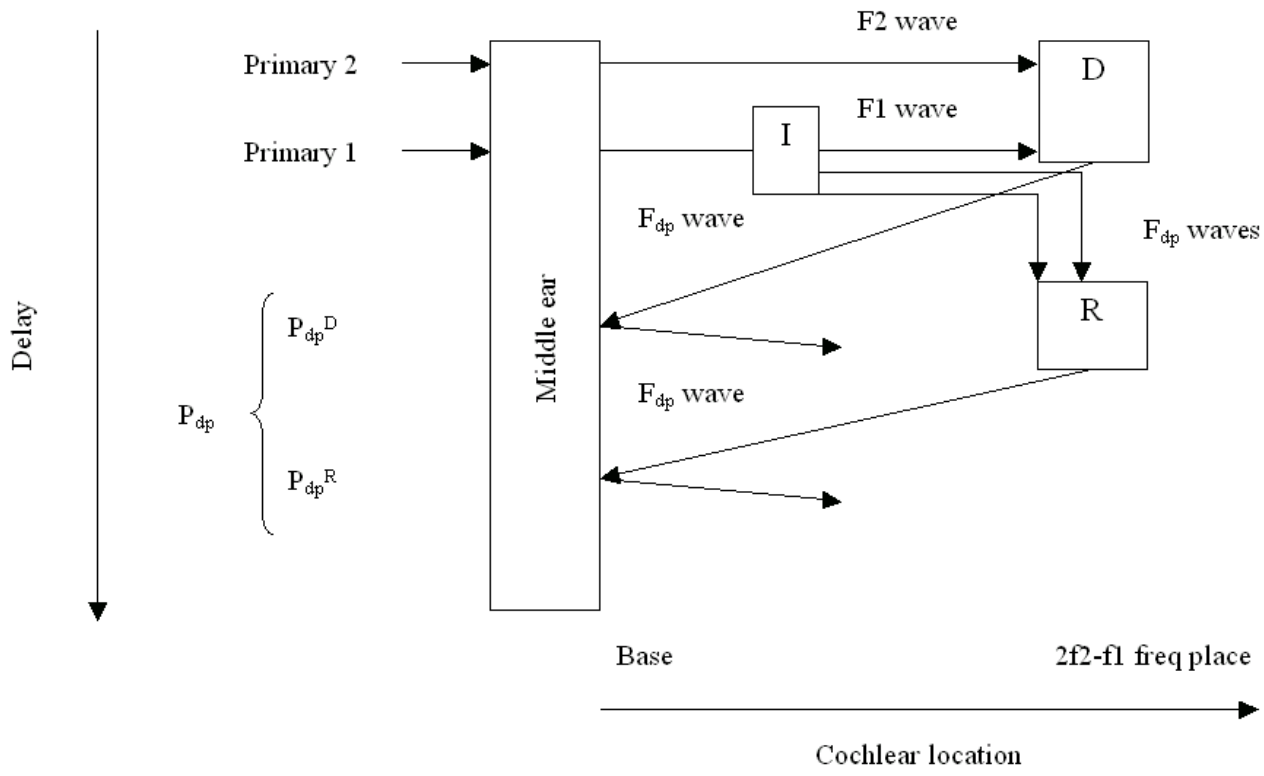

Figure 1.11 Theorised mechanism of generation of the 2f2-f1 DP. Distortion (D) and reflection (R) are generated at the 2f2− f1 frequency place. Distortion generates a DP frequency wave that travels toward the cochlear base. Waves of the DP frequency, the result of BM imperfections (I), slow as they arrive at the DP frequency place and are subsequently reflected toward the cochlear base. Source: Wilson and Lutman, 2006.

The source of the 2f2− f1 DP is still not entirely known, as the two components (non-linear distortion and reflection) may originate at the 2f2− f1 frequency place or with the wave-fixed component being basal to the 2f2− f1 place. It is clear that further investigation of the 2f2− f1 distortion product is necessary.

1.6.4 Somatic electromotility and non-linearity

Another issue that has been highlighted concerns how the non-linearities associated with stereociliary transduction and the somatic electromotility of OHCs mix with one another to produce OAEs (Robinette and Glattke, 2007).

There is still much controversy over the origin of this non-linearity and to date many hypotheses exist: 1) mechano-electrical transduction by stereocilia, 2) electromechanical transduction by somatic motility, 3) mechanical non-linearities resulting from ion channel processes (Liberman et al., 2004). The discovery of prestin, the motor protein located in the OHC of the cochlea corresponded with numerous investigations to evaluate its function (Cheatham et al., 2005). Current issues have arisen concerning the role of prestin (Liberman et al., 2004). To properly link OHC electromotility with the amplification processes, frequency selectivity needs to be assessed and the completeness of the OHCs transducer discovered (Cheatham et al., 2004).

By using similar techniques Liberman et al. (2004) and Cheatham et al. (2004) revealed that although 2f1− f2 distortion components are reduced, they are still present in the cochlear microphonic potentials in the ear canal of prestin knockout mice. Cheatham et al. (2004) discovered that compound action potentials in prestin knockout mice are similar to those in the controls at high levels where the cochlear amplifier has little influence.

1.6.5 Pressure waves

Olson (1999) provided direct evidence of intra-cochlear pressure waves close to the partition, indicating a fluid component to the cochlear wave. Olson (1999) describes

the frequency and location dependence of the non-linear fluid wave. Variations in pressure were used by Olson (1999) to find the velocity. The waves penetration depth was approximated to be 15 μm. This indicates the quantity of fluid within the wave, its magnitude and frequency dependence. The results were obtained in anaesthetised gerbils. In the experimental conditions one location along the cochlear partition was probed in the scala tympani. Gains measured were up to 50 dB recorded at the scala tympani relative to the ear canal (Olson, 1999). It is difficult to know if the probe alters the mechanics and how the BM and fluid motion can be disentangled. Differences in pressure variations result in the conclusion that there is fluid motion, and the quick decline in pressure associated with increasing distance corresponds with the localised nature of the TW.

1.6.6 A few further criticisms

A criticism of Ren et al.'s (2006) investigation is that only the high frequency region of the BM could be studied using the interferometer.

An issue with Ruggero's (2000) investigation was that measurements were made on different species; this has implications, as it may not be appropriate to compare DPOAEs elicited in gerbils and guinea pigs.

Different hardware systems used in obtaining OAE measurements have different methods so are difficult to compare (Suckfull et al., 1996). Even in the non-pathological ear DPOAEs can vary by a large degree, because of probe position, external and middle ear characteristics and due to the influences of spontaneous otoacoustic emissions.

1.7 Aim of Research

Current understanding regarding the origin of distortion product otoacoustic emissions (DPOAEs) suggests that they arise via two distinct mechanisms. One mechanism is thought to be non-linear distortion, and the other being linear-coherent reflection. These two components combine and contribute to the DPOAEs measured

in the ear canal. This mechanism-based taxonomy is founded on experimental evidence. Each mechanism has different delay characteristics. This allows investigators to distinguish the mechanisms via time window separation. Another method allows the mechanisms to be separated via the introduction of a suppressor tone. In a recent publication it was confirmed that not only are these two components evident in the 2f1− f2 DPOAE, but also in the 2f2− f1 DP. This casts doubt on the existing model. The two separation techniques will be compared for the 2f2− f1 DP in order to challenge the existing theory.

Wilson and Lutman (2006) investigated the mechanisms of generation of the 2f2− f1 DP in humans using a time-window separation method. Wilson and Lutman (2006) proved that in most participants (18 of 20) both a wave-fixed and a place-fixed component are present in the 2f2− f1 DP. The authors also demonstrated that the 2f2− f1 emission is adequately measurable above the noise floor. Sharp (2007) also separated the two components for the 2f2− f1 DP, but stressed the need for future research.

It has been demonstrated that there are still large gaps in our knowledge regarding the understanding of DPOAEs. One issue focuses on the lack of understanding surrounding the mechanisms of generation of the 2f2− f1 DP. There is now some evidence indicating that the locus of origin of the 2f2− f1 DP is different from that of the 2f1− f2 DP, and that it potentially propagates in a different way. Experimental investigations have revealed much concerning the components of the 2f1− f2 DP; using time window separation and suppression techniques. A further investigation will implement these techniques with the 2f2− f1 DP, in order to evaluate if the current two-mechanism model holds true. The following investigation will utilise a fixed frequency ratio, but will alter suppressor tone level and frequency in order to investigate the current two-mechanism paradigm. This will challenge existing theory and broaden the understanding of a presently under-studied DP.

1.8 Statement of hypotheses

Time window separation techniques and the suppression method will separate the 2f2− f1 DP into two separate components, located above the noise floor. As the suppressor level increases, the effect on the DP will increase. The relating null hypothesis is that the two techniques will not separate out the 2f2− f1 DP into distinguishable components or the components will not be significantly above the noise floor.

Also as the suppressor frequency and intensity alter, the effects on the DP will alter. The relating null hypothesis is that as the suppressor frequency and intensity alter, there will be no noticeable effect on the DP.

CHAPTER 2: RESEARCH DESIGN

2.1 Introduction

The previous chapter described the present theories regarding the origins of DPOAEs. The two-mechanism theory was described in detail, whereby DPs arise through non-linear distortion and linear coherent reflection (Shera, 2004; Kemp, 2002). The techniques used in verifying this theory have been described.

It was emphasised however, that until recently few investigators have studied the origins of the 2f2− f1 DP. There are still many unknowns surrounding this DP, not least if the 2f2− f1 DP has a different locus of origin to the 2f1− f2 DP, and if it propagates in a different way. The aim of the present investigation is to:

- Determine whether the 2f2− f1 DP is accurately measurable above the noise floor.
- Determine the effect of suppressor level on the 2f2− f1 DP.
- Determine the effect of suppressor frequency on the 2f2− f1 DP.

This will challenge existing theory and broaden the understanding of a presently under-studied DP, potentially allowing inference of where the 2f2− f1 DP is generated.

This section will explain the methodology implemented for the selection of participants and the practical considerations taken into account whilst conducting this investigation. The entire investigation was conducted in the Institute of Sound and Vibration Research (ISVR), University of Southampton. All procedures took place in a sound proof booth in accordance with ISO 8253-1 for the measurement of hearing threshold to a level of 0 dB HL.

2.2 Participants

2.2.1 Recruitment

A total of 23 participants took part in this investigation. They were recruited from within the Institute of Sound and Vibration Research (ISVR), and other schools from within the University of Southampton. Participants were aged between 19-32 years. This was to ensure against the selection of participants with damaged hair cells, as this may have consequences for the generation of DPOAEs (Oeken et al., 2000; Lonsbury-Martin et al., 1991). The experimental procedure was conducted throughout July-August, 2010.

Participants were chosen only after intensive screening. All participants were required to have otologically normal ears. Selection criteria adhered to ISO 389 (2000) and the definition of normality stated within. Participants were all of normal health. It was attempted to include an equal number of males and females, but this was unfeasible at the time of testing. Requirements of all participants included no history of tinnitus and it was essential that they were not exposed to loud sounds within 48 hours prior to the session beginning.

Participants were excluded if they had ears deemed to be pathological. This was determined through taking a history to evaluate issues such as past ear surgery, ear disease, and/or persistent infections. No participants were included if they had a known family history of hereditary deafness. Participants were screened via the following procedures:

- History taking.

- Otoscopy: In order to check for excessive wax or occlusion in the ear canals, including foreign bodies. To look for otitis media with effusion. To evaluate if there was an incidence of otitis externa or any other contraindications (BSA, 2010). Otoscopy was performed based on the BSA protocol (BSA, 2010).

- Tympanometry: Results must of been within the normal range expected for an adult with healthy middle ear function:

Measurement	Normal Range
Ear canal volume	0.3 - 2.0 ml
Middle ear compliance	0.3 - 1.6 ml eqv
Middle ear pressure	–50 - +50 daPa

This was to ensure normal middle ear function. Tympanometric investigation was performed using a GSI-33 tympanometer in diagnostic mode, utilising 226 Hz frequency and swept at + 200 to – 200 daPa. Tympanometry was performed according to the BSA protocol (BSA, 1992).

- Audiometry: Following the BSA protocol (BSA, 2004) a full audiometric assessment was conducted, inclusive of octave intervals from 0.25 to 8.0 kHz. This was carried out using a Kamplex 3 audiometer with TDH-39 headphones. This was to ensure hearing thresholds were within normal limits of + 20 dB HL, as DPOAEs appear to be related to cochlear integrity, which has been correlated with hearing threshold (Boege and Janssen, 2002; Gorga et al., 2003).

- A health and consent form was completed by all participants prior to the session beginning in order to support the history, determine any exposure to loud sounds or ototoxic substances, and rule out any severe trauma to the auditory system.

The investigation protocol was approved by the ISVR Safety and Ethics Committee, and all potential hazards were evaluated through Risk Assessment forms.

2.3 Procedure

A brief history was taken, before an ear examination (otoscopy). Tympanometry was then performed, followed by audiometry. Participants then completed a health and consent form. The test session could then begin in full.

2.3.1 Equipment and test configuration

All procedures were carried out within ISVR, University of Southampton. The Investigation was conducted specifically in Audiometric Booth 1. The basic set-up is indicated in Figure 2.1.

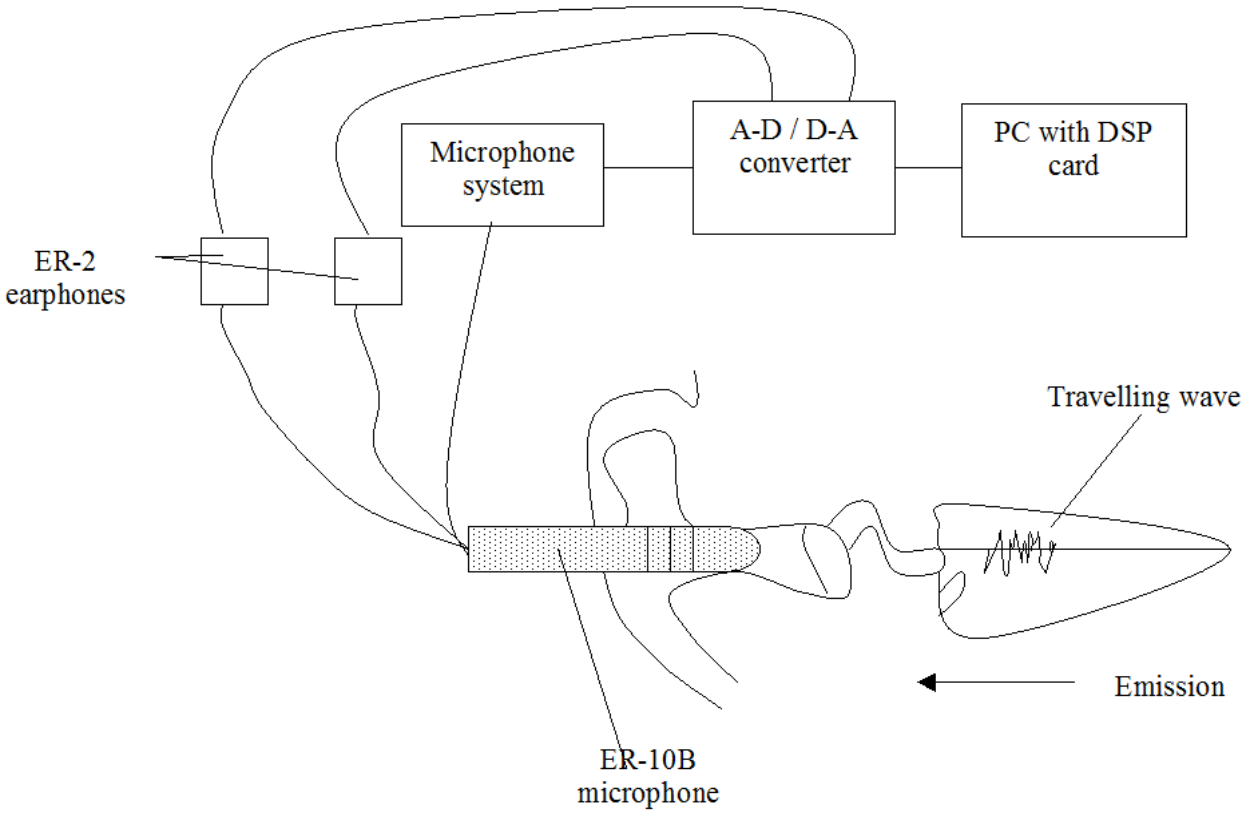

Figure 2.1 Basic procedural set-up for the recording of a DPOAE in the laboratory. Source: adapted from Lonsbury-Martin and Martin, 1990, and Wilson, 2005.

Equipment consisted of a Personal Computer with a Digital Signal Processing card linked to an external analogue-digital (A/D) and digital-analogue (D/A) converter unit (Institute of hearing Research DSP remote converter module), at a sample rate of 32.768 kHz. The stimuli were delivered via ER-2 insert earphones (Etymotic Research) connected to a common probe (Etymotic Research ER-10B+ OAE probe). The probe was sealed in the ear of the participant using a standard tympanometry probe tip. The size of probe tip was chosen based on the size of the participant's ear

canal. A new probe tip was used for each individual to protect against possible cross contamination. The probe was placed in the ear such that it needed no external support to stay in the ear. The probe contained a microphone to measure the sound pressure level in the ear canal. The two tubes were positioned such that one just protruded from the entrance of the probe tip, and the other was flush with the entrance. This has been considered to be the best position for stimulus delivery (Lineton, pers comm.) The output was amplified by 40 dB using the ER-10B+ system and fed to the A/D converter and stored by the DSP card. Epochs of 62.5 ms were gathered and transformed to the frequency domain via FFT. Measurements of phase were collected in degrees and amplitude in dB. Data was visually output onto a Desktop personal computer (PC) monitor.

2.3.2 Test sessions

All testing was conducted in a single session. Each test session was designed to last approximately one and a half hours. This duration caused minimum disruption to the participants, whilst enabling the investigator to collect all of the relevant information. By conducting the investigation in a single session issues of probe fit and individual variation were reduced (Zhao and Stephens, 1999). The participants were instructed not to create any noise or move about throughout the duration of the test. Participants were informed that doing so would disrupt the test. Participants were sat in a comfortable recliner chair, and were informed that the lights could be switched off if they found this more relaxing. This would not interfere with the results. The investigator viewed the participant at all times through an observation screen. Participants were informed to raise a hand if they needed a comfort break or wished to communicate in any way. A glass of water was provided for all participants.

The ear with the best pure tone thresholds was selected from each participant for testing. If there was no difference between ears, an ear was randomly selected.

In order to ensure complementary analysis the following parameters were chosen based on the investigations of Wilson and Lutman (2006) and Sharp (2007). It is important to note that these previous investigations were both conducted within ISVR,

Univeristy of Southampton, and the same equipment and facilities were used as in the present investigation.

2.3.3 Parameters

Wilson and Lutman (2006) used four frequency ratios, f2/f1 = 1.05, 1.1, 1.22 and 1.32. In the present study a frequency ratio of 1.05 was used as this revealed the largest 2f2− f1 DP in Wilson and Lutman's (2006) investigation. Under this condition the DP was situated furthest above the noise floor, as indicated in Figure 2.2.

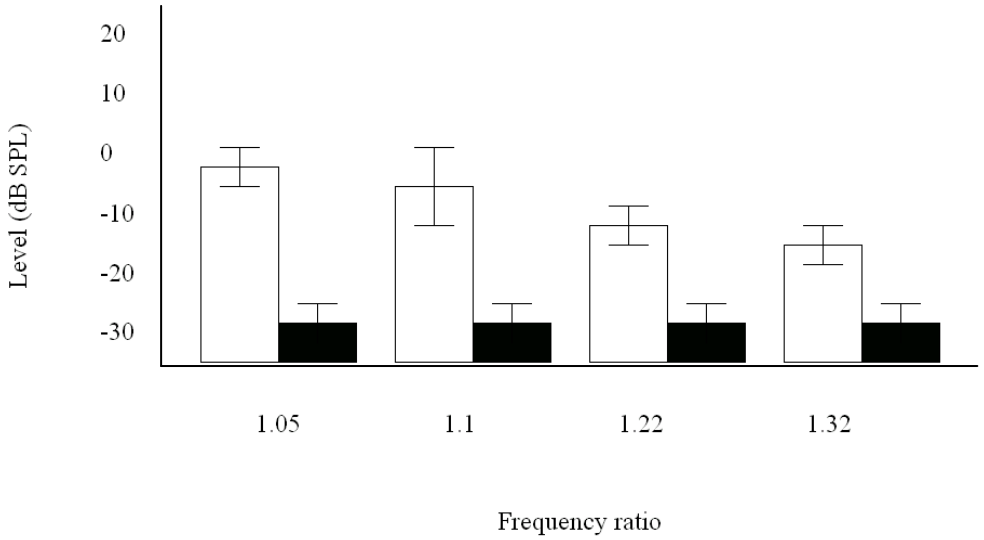

Figure 2.2 The 2f2− f1 emission (white bars) and corresponding noise level (black bars), averaged across participants. L1 = 65 dB, L2 = 60dB, and L1 = 55 dB, L2 = 40 dB SPL (with f2/f1=1.22). Error bars represent one standard deviation. Source: Wilson and Lutman, 2006.

DPOAEs were measured using a maximum buffer level of 50, averaging the 65.2 ms epochs. The rejection level was set at signal-to-noise ratio > 10 dB over the frequencies of interest. The levels of the primary tones were L1 at 65 dB and L2 at 55 dB SPL. Other primary tone levels have been utilised in the past such as L1 = 55 and L2 = 40 dB SPL by Kummer et al. (1998) and L1 = 60 and L2 = 45 dB SPL by Kalluri and Shera (2001). Once again the levels chosen in the present investigation were selected to ensure consistency with the investigations carried out by Wilson and Lutman (2006) and Sharp (2007). These primary levels were deemed adequate to

elicit an appropriate 2f2− f1 DP, as they are barely measurable at lower levels (Wable et al., 1996).

By adding a suppressor tone with a frequency near to the DP, models predict that it will have a greater influence on the reflection site component than the non-linear distortion component (Talmadge et al., 1999; Kummer et al., 1995; Kalluri and Shera, 2001). Thus it is envisaged that the levels of both these mechanisms may be altered by introducing a suppressor tone. At low suppressor levels there will be minimal effect. As the suppressor tone increases in level its influence on the reflection component will also increase and the overall level of the DP will decline.

The influence of the frequency of the suppressor will also be studied. As the suppressor tone moves location closer to the DP it should become more effective at suppressing the reflection component. Another variation on this is to change whether the suppressor is located above or below the DP. It was suggested by Sharp et al. (2007) that locating a suppressor between the DP and the primaries will lead to a greater amount of suppression than when the suppressor is outside the two components. Gorga et al. (2002) demonstrated steeper slopes of DPOAE decrement versus suppressor level function for the situation in which f2>f3 relative to f2<f3, where f3 is the suppressor frequency.

The recording conditions are highlighted in Table 2.1. DPOAEs were initially measured via a sweep recording with a minimum buffer level of 50, and a maximum of 200. Either a low frequency sweep centred on 2 kHz (1.75-2.25 kHz) was studied first, or a high frequency sweep centred on 4 kHz (3.75-4.25 kHz). These sweeps were chosen to encompass both a low and high frequency region. The F2 was swept in frequency in 16 Hz increments. An automatic stopping mechanism was activated at signal-to-noise ratio (SNR) of 15 dB. From this sweep a single frequency was chosen for further analysis. This was the point with the greatest SNR across the range of f2 values, based on visual inspection of the data. This was to ensure that the analysis was based on robust pairs of data that were not contaminated by noise.

Table 2.1 Recording conditions that each individual participant received. The suppressor level was varied through 0, 20, 40, and 60 dB SPL for each condition.

The f2/f1 = 1.05, whereby L1 = 65 dB, L2 = 55 dB SPL. The High frequency region represents 3.75-4.25 kHz, and the Low frequency region 1.75-2.25 kHz. The order of testing was determined by a Latin Square method. Each condition was repeated. Suppressor frequency (Hz) is relative to DP frequency.

Suppressor Frequency	2f1– f2		2f2– f1	
	Low	High	Low	High
–32	X	X	X	X
–16	X	X	X	X
16	X	X	X	X
32	X	X	X	X
48	X	X	X	X
64	X	X	X	X
None	X	X	X	X

The primaries resulting in this DP were used for the analysis of suppression. The single data had a maximum buffer level of 500 and a minimum of 200. There were 24 recording conditions for each participant. Measurements were initially made with no suppressor tone added and the level of the DP was recorded. Throughout suppression all variables, including primary levels, primary frequencies, and rejection levels remained unaltered. The same measurement was then made but with a suppressor tone introduced 32 Hz below the DP, and the amplitude of the DP was again recorded. The suppressor tone was introduced through the same channel as f1, and presented through the same ER-2 earphone. It was attempted to deliver the suppressor through a separate channel, via a real ear measurement (REM) probe, but it was not possible to synchronise frequencies sufficiently accurately. The suppressor was first introduced at 20 dB, and this level was raised in 20 dB increments, to a maximum of 60 dB, in order to study the influence of suppressor level on the DP. These levels were selected based on the work of other investigators such as Talmadge et al. (1999), Gaskill and Brown (1996) and Kummer et al. (1995) in order to show the effect of the suppressor tone having no influence on the DP (lower suppressor levels) to completely removing it (higher suppressor levels). This process was repeated for suppressors located from –32 Hz to + 64 Hz above the DP place, in 16 Hz increments.

As a reference for the unsuppressed level of the DP, a measurement was made with no suppressor introduced. The location of the suppressor tones relative to the DP can be seen in Figure 2.3.

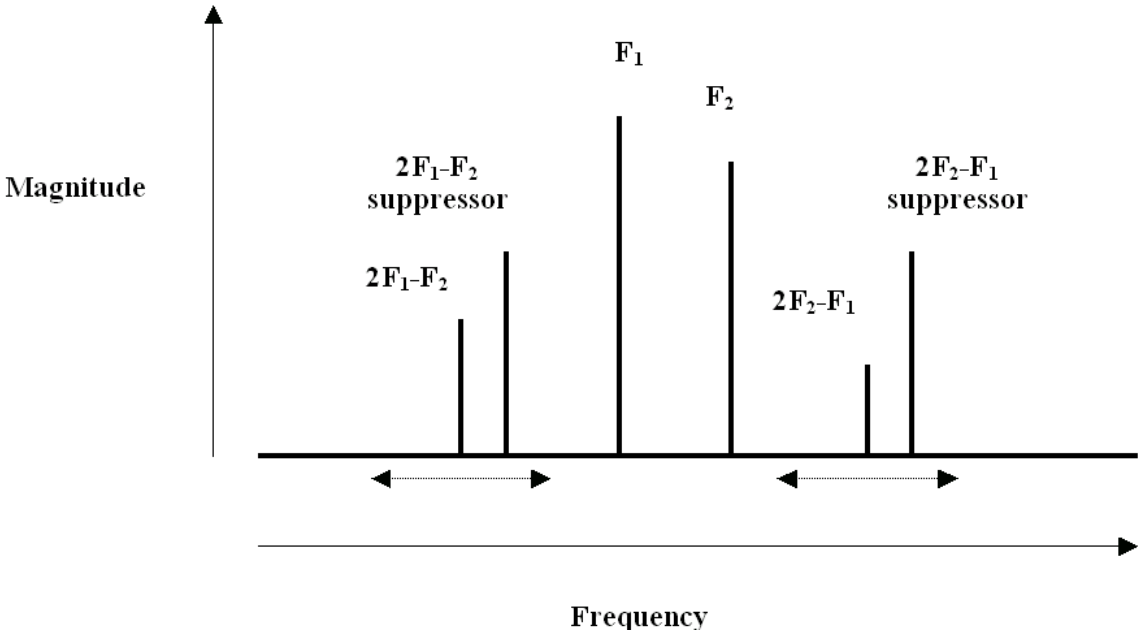

Figure 2.3 Two DPOAEs represented in the frequency domain, highlighting the two eliciting primary tones (F1 and F2) and the corresponding DPs of interest. The location of the suppressor tones are also included. The dotted arrows indicate the region of location of the suppressors. In this example the suppressors are at a positive relative frequency. Source: adapted from Sharp, 2007.

The exact procedure was then repeated in order to ensure test re-test reliability. This reinforces the validity of the results.
The same procedure was then carried out for the alternative DP (either 2f1− f2 or 2f2− f1). This was then repeated over the alternative frequency region (high or low).

The order of testing was randomised between participants by the application of a Latin Square. This was to protect against order effects and other variations in hair cell activity, such as acclimatisation as the participant moves from a loud external environment to a sound controlled environment.

It was deemed important to also study the 2f1− f2 emissions again as this also aids in validating the reliability of the experimental set up.

2.3.4 Calibration

The experimental set up was calibrated utilising an audio frequency spectrometer, which was coupled to an IEC-711 ear simulator. A tympanometry probe tip was attached to the device and inserted into the ear simulator. The earphones were then calibrated individually from 256 Hz to 6000 Hz in 256 Hz increments at a level of 60 dB, at a resolution level of ±0.5 dB. Adjustments were made directly to the stimulus levels. Intermediate frequencies were adjusted by linear interpolation. The microphone was calibrated only at 1024 Hz because of the potential influence of standing waves at higher frequencies and the discrepancies in the responses because of possible differences in probe tube insertion (Wilson and Lutman, 2005). The frequency response is expected to be linear across the range of frequencies investigated, based on its specification and manufacturer's individual calibration curve, so the individual result of the 1024 Hz was applied across the whole frequency range.

2.4. Data processing

2.4.1 Programme

Data processing was conducted utilising Matlab (Mathworks Inc.) software. A pre-existing program initially used by Parazzini (2004) and adapted further by Wilson and Lutman (2006) was implemented in this investigation. The programme was modified in order to allow adequate processing of the data found within this investigation.

The raw data is fundamentally processed in two stages in order to transfer it into a format suitable for further analysis.

The collected data is of a form in which both wave and place-fixed components of the DPOAE are combined across an f2 frequency sweep in 16 Hz increments.

The initial stage involved phase unwrapping. This allows the transformation of data with rotating phase (from -180 to +180°) to data with a continuous phase variation with frequency (Knight and Kemp, 2000). This is achieved using a phase unwrapping algorithm.

The following stage requires the data to be converted into the time domain. This enables the two components (wave-fixed and place-fixed) to be separated in order to compare the individual component amplitudes with that of the total DPOAE. The two components are separated according to their latency (Knight and Kemp, 2000) as the wave-fixed component has a shorter latency (≤2 ms) than the place-fixed component.

After separation of the components they are converted back into the frequency domain, and power averaged in order to give a single amplitude value for that component.

The Matlab code for both stages is reproduced in Appendix 1.

2.4.2 Stage 1: Data formatting and phase unwrapping

This programme reads the files (.dat) from the DPOAE recording software. The phase data is unwrapped and the required data components are used for further processing.

2.4.3 Stage 2: Un-mixing

Stage 2 carries out time window separation according to the method of Withnell et al. (2003):

1) The conversion of the DPOAE amplitudes into a complex form.

2) Equal frequency spacing between the data points is achieved via linear interpolation (Wilson, 2005).
3) The data is extended by zeros in order to attain a value that is a power of two (this helps the FFT calculation).
4) An inverse fast Fourier transform (IFFT) is conducted on the data.
Results are exhibited as a plot in the time domain for checking.
5) In order to remove the reflection component of the DP, leaving only the distortion component, the IFFT is subjected to a recursive exponential filter (order 10) with a cut-off at 2ms. Kalluri and Shera (2001) further supported the cut-off time as they unveiled that for the 1-2 kHz range, reflection emissions are delayed by approximately 15 periods of the stimulus frequency (Wilson, 2005).
6) The filtered IFFT is subjected to a FFT to obtain the sweep corresponding to the complex amplitude of the wave-fixed component. This is displayed as a plot of the distortion (wave-fixed) component.
7) The subtraction of the wave-fixed component from the original complex amplitude data reveals the place-fixed (reflection) component. The place-fixed data is plotted on the same axes as the wave-fixed data (Wilson, 2005).

The programme output also features plots of the original complex amplitude data in the time domain and the phase and amplitude of both the wave-fixed and place-fixed components in the frequency domain.

2.4.4 Averaging

The previously described un-mixing presents the data as a range of amplitudes across frequency. It is useful to obtain a single amplitude value for each of the recording conditions. This is done by averaging across frequency, achieved by power averaging (Knight and Kemp, 2001; Beckerleg, 2002; Wilson, 2005; Sharp, 2007).

2.4.5 The noise floor

A method of noise floor estimation was utilised as developed by Wilson and Lutman (2006), and further used by Sharp (2007). Once again, Matlab was used in order to

process the noise. This programme was similar to those used for processing the emission data.

Background noise measurements were obtained near to the DP frequencies whilst measuring the DPOAE. The phase data of the noise was not measured at this point. Instead, the recorded amplitudes were labelled with a random phase, as it can be assumed that the phase of the noise is independent of frequency (Wilson, 2005). The subsequent phase and amplitude values obtained for the noise were then subjected to the same processing techniques as the DPOAE data, and averaged. This created individual estimates of the noise in the two latency periods for each recording for each participant (i.e. wave-fixed and place-fixed). Consequently the DPOAE and noise data could be analysed directly in order to reveal whether the emissions were significantly above the noise.

2.5 Statistical design and analysis methods

Statistical analysis of the data was conducted using a combination of SPSS 17 (Lead technologies Inc.) and Microsoft Excel.

The first stage in the analysis of the results was to determine whether the pattern of results obtained demonstrated a normal distribution. In order to achieve this aim the Kolmogorov-Smirnov test was implemented on both the DP recordings and corresponding noise levels. This process is essential in determining the use of parametric testing (Field, 2009).

The DP and corresponding noise recordings were then analysed to ensure the validity of the results. The DP should be sufficiently distinguishable above the noise. This was achieved by visual observation of graphed data, and via Student's t-tests. The t-test output also displayed confidence intervals.

The ultimate goal of the investigation was to determine the influence of the suppressor level and position on the 2f1− f2 DP and how this compares to the 2f2− f1 DP. This was achieved through visual analysis of suppression-growth functions, and

statistically via repeated measures analysis of variance (ANOVA). Post hoc tests (Bonferroni) were then carried out to determine where the significant differences specifically lay.

The results are presented in the following chapter.

CHAPTER 3: RESULTS AND ANALYSIS

3.1 Introduction

3.1.1 Participants

A total of 23 participants were initially recruited for testing. Of these original 23 participants three were excluded, due to their age ranges exceeding the recommended for testing. The participants included seven males and 13 females, with a mean age 23.6 years, and a standard deviation of 2.6 years. Hearing thresholds were all within normal limits and no contraindications were exhibited.

3.2 Emissions

3.2.1 Recorded emissions (prior to processing)

Each participant underwent each recording condition, for both the 2f1− f2 and 2f2− f1 DPs. DP levels were recorded along with the corresponding noise level. A sweep measurement was first obtained in order to determine the most appropriate primary frequencies to elicit the best DP response. This was based on the SNR. Single recordings were then made, initially with no suppressor, and then with a suppressor introduced.

The suppressor frequency was altered from 32 Hz below the DP to 64 Hz above, in 16 Hz intervals. Suppressor level was gradually increased for each suppressor position, from 0 dB to a maximum of 60 dB in 20 dB increments. Where erroneous results were evident at the highest suppressor level, a suppressor was introduced at 55 dB, as opposed to 60 dB, in order to elicit a clearer signal. This occurred most frequently for the 2f1− f2 low condition. Results were deemed erroneous where upon visual inspection the data point was located significantly far away from the other data points.

The recorded sweep data were then power averaged in order to obtain single values for amplitude. A similar process was conducted on the noise values. Figures 3.1 and 3.2 below show that the average DP level was well above the average noise in all conditions before processing. The figures indicate that the 2f1− f2 DP is higher than the 2f2− f1 DP, and that both DPs are above the noise.

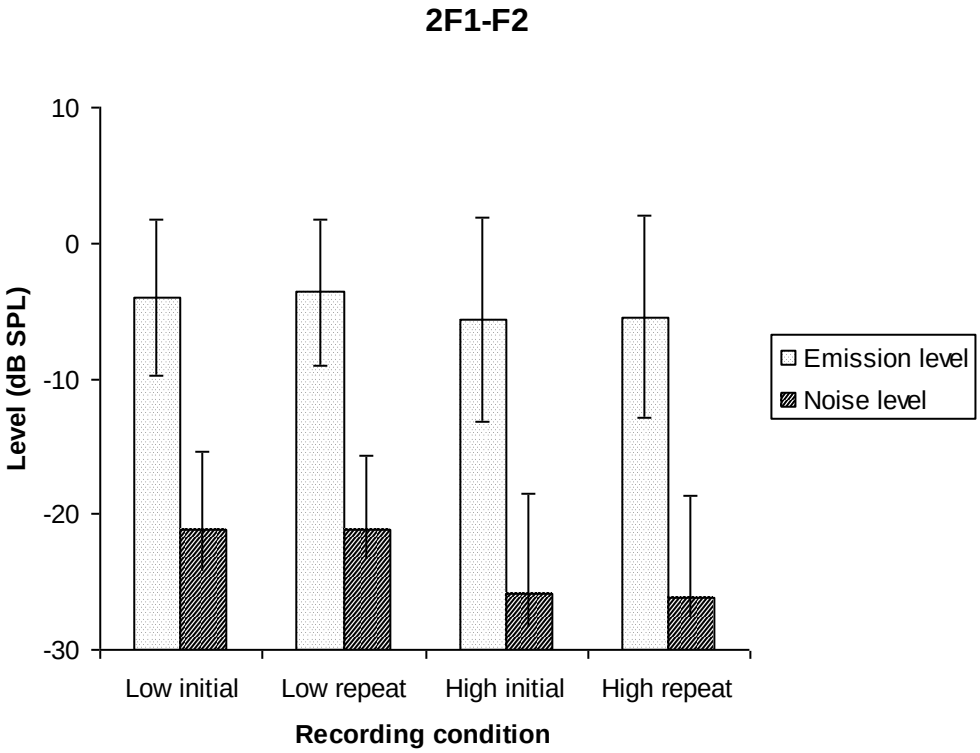

Figure 3.1 2f1− f2 DP and noise levels averaged for all 20 participants. Both the low and high recording conditions are shown, along with the initial and repeat recordings. The error bars represent a single standard deviation.

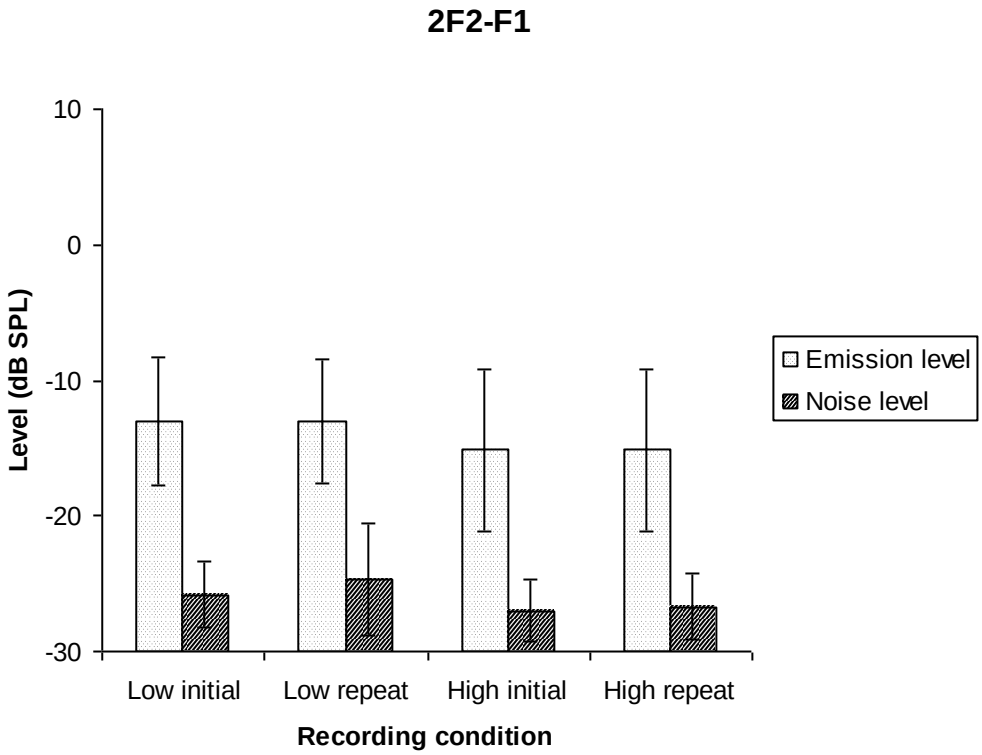

Figure 3.2 2f2-f1 DP and noise levels averaged for all 20 participants. Both the low and high recording conditions are shown, along with the initial and repeat recordings. The error bars represent a single standard deviation.

3.2.2 Emissions (post processing)

The technique by which the initial data were processed has been described previously. Processing was carried out using the Matlab software. The initial stage involves a procedure known as an inverse fast Fourier transform (IFFT). Knight and Kemp (2000) describe how the two components of the DPs can be identified based on their group delays. Similar to the results of Knight and Kemp (2000), here it was also demonstrated that there is a peak seen before approximately 3 ms, followed by a number of peaks thereafter. An example of the results obtained from a participant from the present study is shown in Figure 3.3. Knight and Kemp (2000) describe that the small group delay corresponds to the wave-fixed emission and the later to the place-fixed emission.

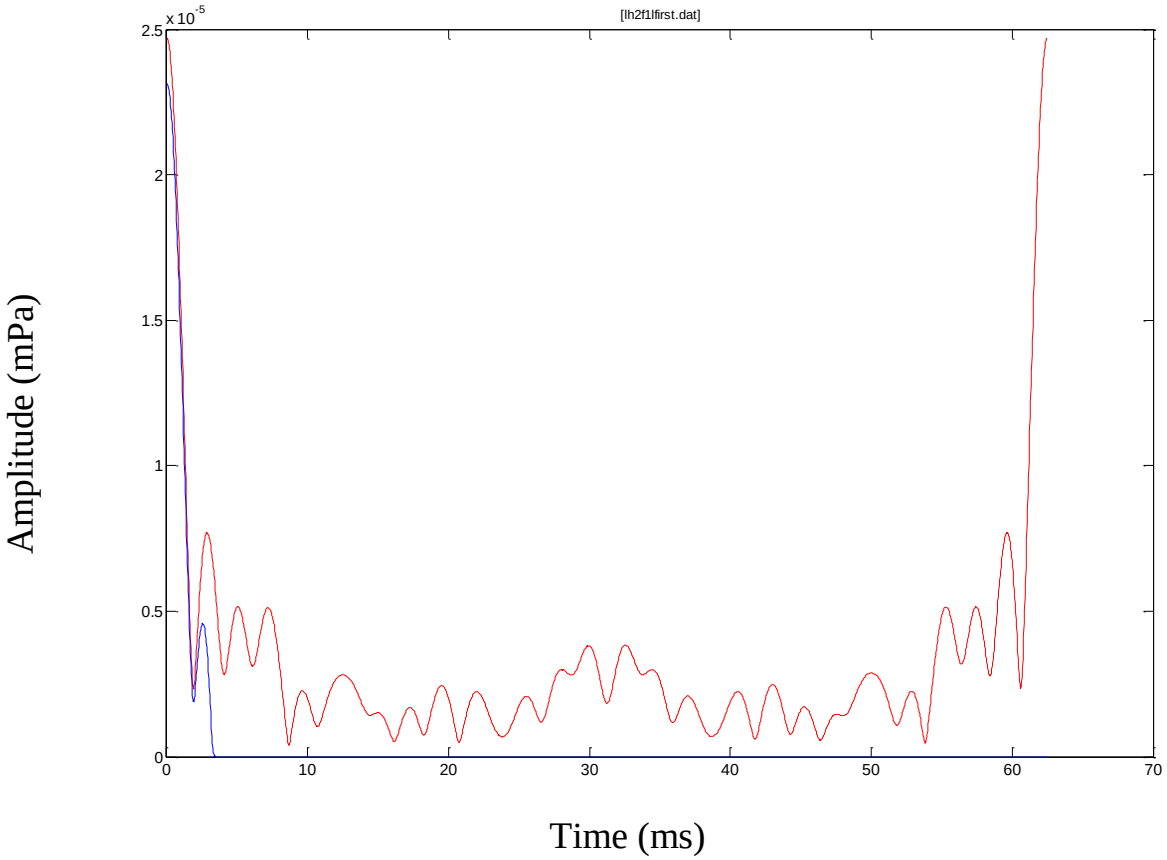

Figure 3.3 Example 2f1– f2 low DPOAE represented in the time domain, as output by Matlab software. Both the wave and place- fixed components are exhibited. This data was obtained from participant LH.

After the IFFT has been performed the phase and amplitude of the DP are displayed. From these plots it is demonstrated that the data contain two components, one with a sloping phase and the other with a steady phase when plotted against frequency. An example is shown in figure 3.4.

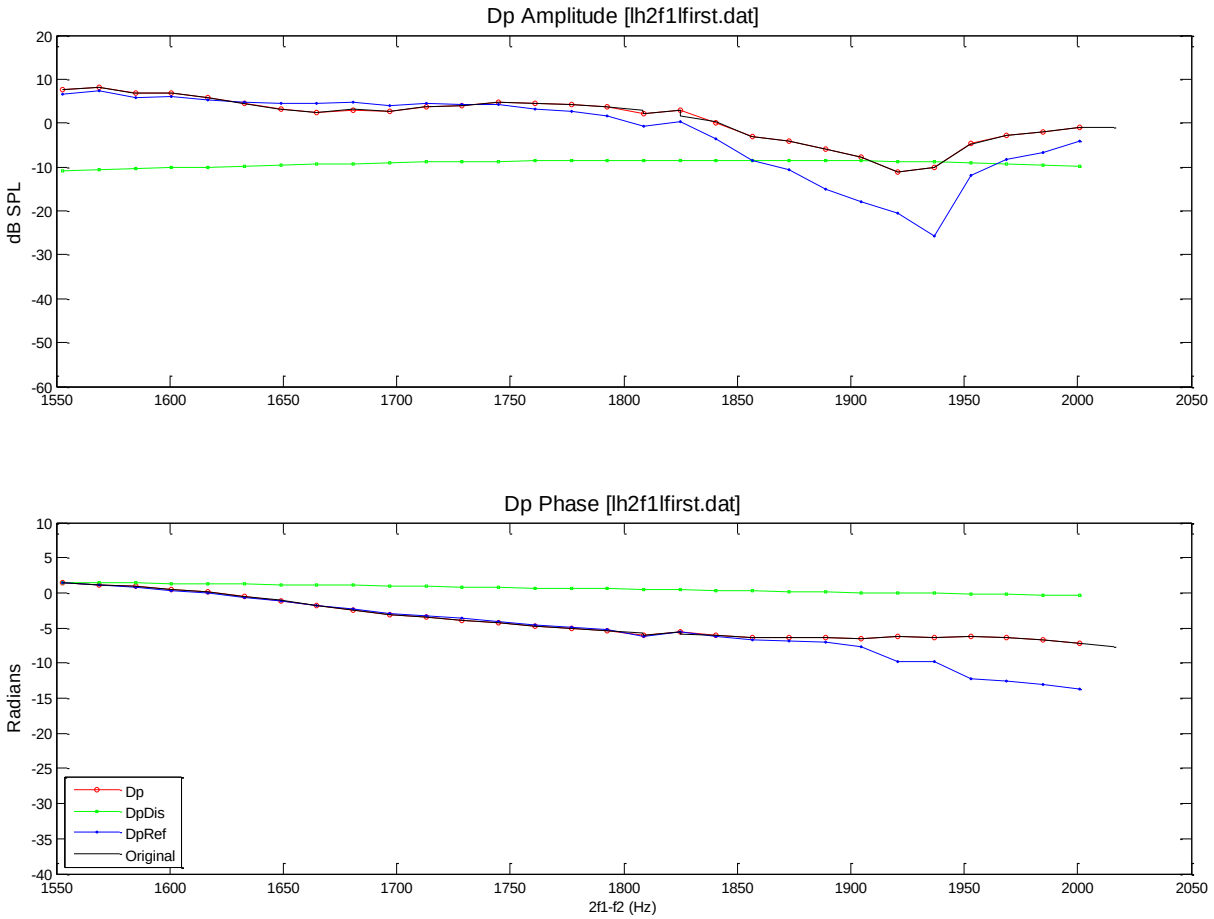

Figure 3.4 Phase (bottom) and amplitude (top) of Fourier transform data from participant LH, for condition 2f1− f2 low initial. The separation of the DP into two components is exemplified. The reflection component exhibits a clear sloping phase and the distortion component has a steady phase.

It is also important to assess that the signal is still above the noise after separation into distortion and reflection components. It is clear from Figures 3.5 to 3.8 that for most of the conditions, when averaged across participants, the signal is above the noise. Once again the 2f1− f2 condition elicits greater levels of DP relative to the 2f2− f1. The reflection component of the DP is greater than the distortion component in both cases. As an example for the 2f1− f2 low initial condition (by comparing Figure 3.5 to 3.6) the distortion component was -17.44 dB SPL (± 7.32 to one standard deviation), and the reflection component was -4.79 dB SPL (± 5.86 to one standard

deviation). The distortion component of the 2f2− f1 DP is particularly low, and there is an overlapping of the error bars between the DPs and the noise.

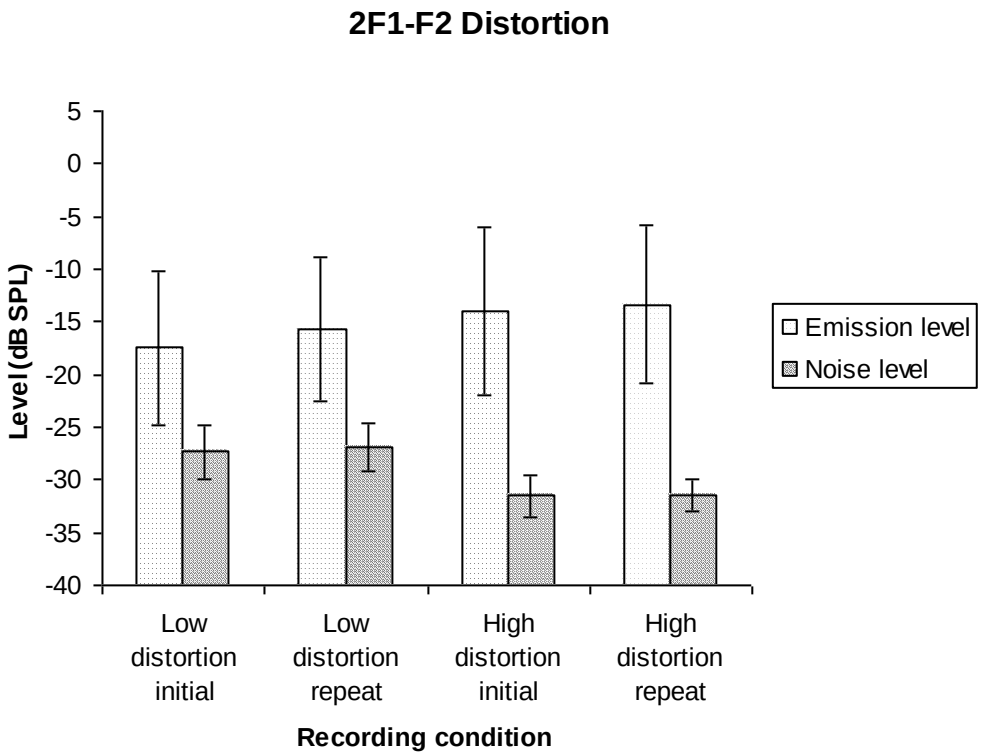

Figure 3.5 2f1− f2 distortion component and noise levels averaged for all 20 participants. Both the low and high recording conditions are shown, along with the initial and repeat recordings. The error bars represent a single standard deviation.

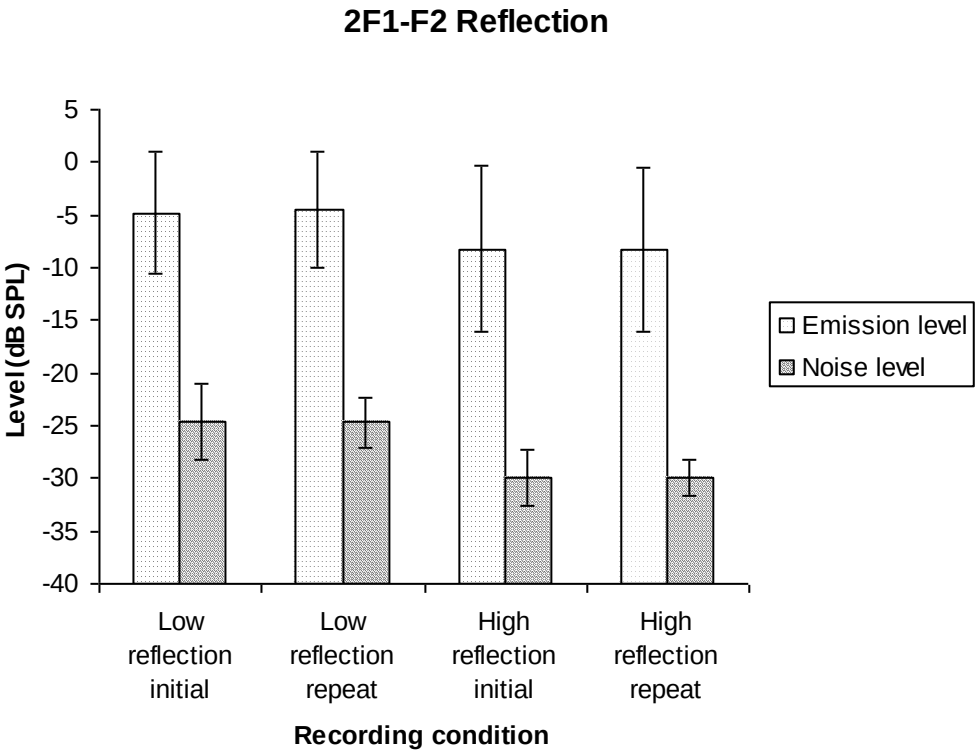

Figure 3.6 2f1– f2 reflection component and noise levels averaged for all 20 participants. Both the low and high recording conditions are shown, along with the initial and repeat recordings. The error bars represent a single standard deviation.

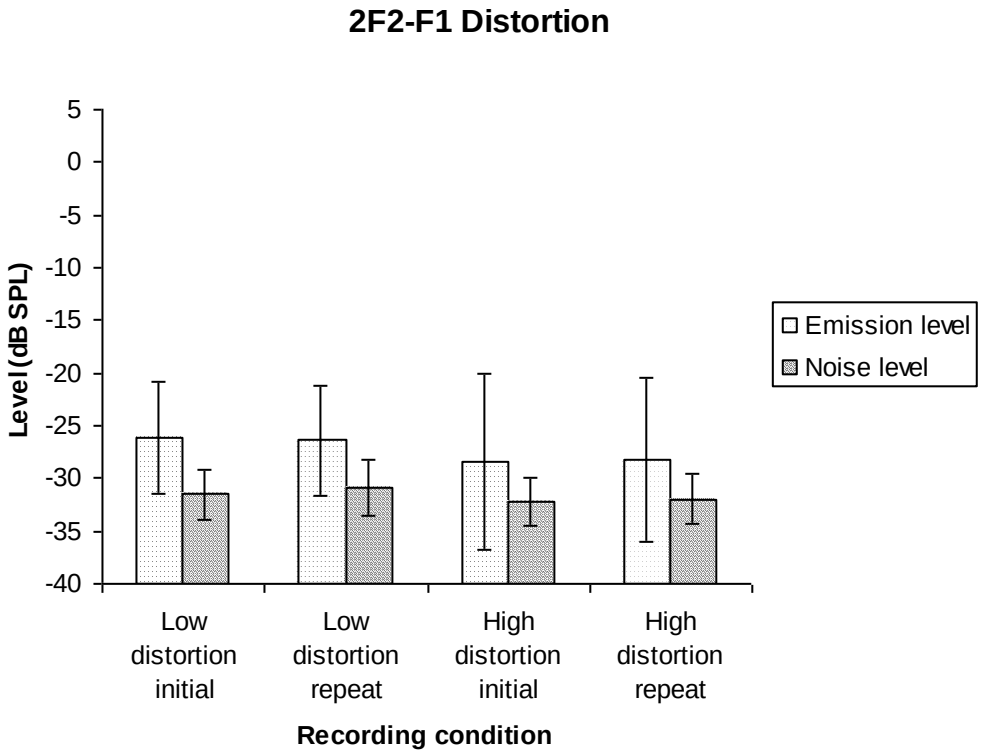

Figure 3.7 2f2− f1 distortion component and noise levels averaged for all 20 participants. Both the low and high recording conditions are shown, along with the initial and repeat recordings. The error bars represent a single standard deviation.

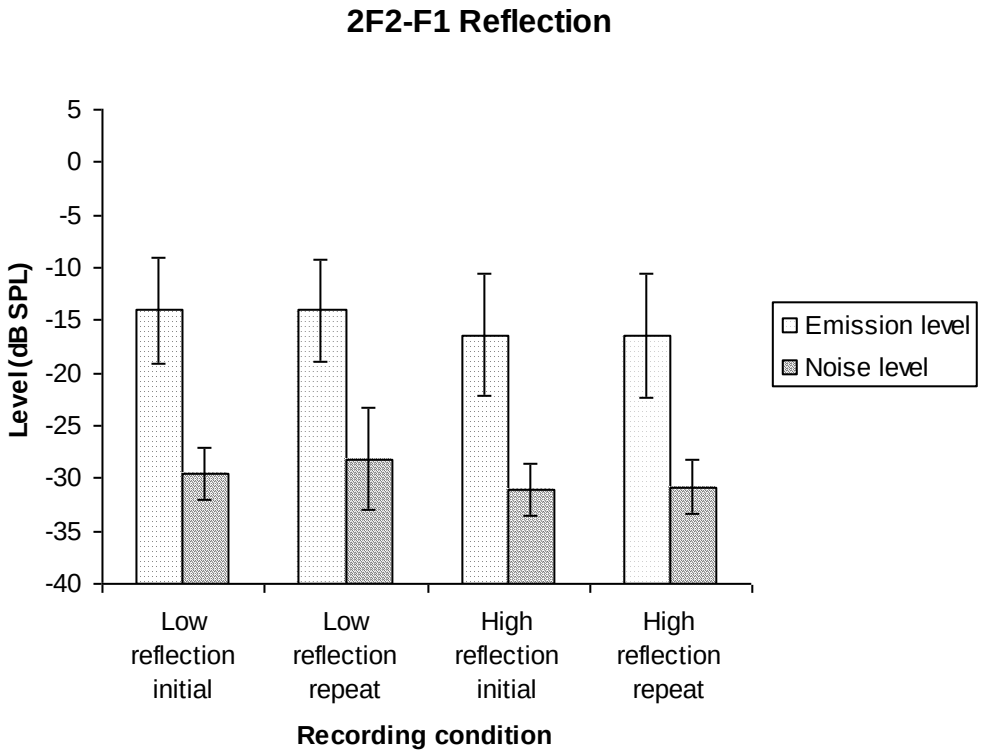

Figure 3.8 2f2− f1 reflection component and noise levels averaged for all 20 participants. Both the low and high recording conditions are shown, along with the initial and repeat recordings. The error bars represent a single standard deviation.

It is also important to determine if after the introduction of the suppressor tone the DP levels are still above the noise. It is shown in Figures 3.9 to 3.16 that the DP levels are above the noise in most conditions after the addition of the suppressor tone. For the 2f1− f2 DP and 2f2− f1 under the high suppression condition it is clear that the noise is large and the error bars are large (as an example for initial mean noise = -14 dB SPL, ± 13.89 to one standard deviation, compared to the mean DP = -2.47 dB SPL, ±7.21 to one standard deviation).

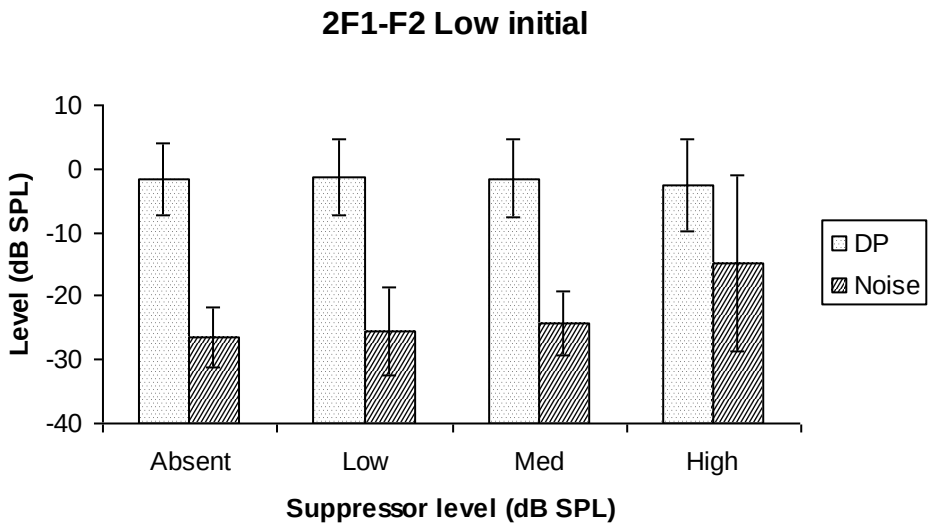

Figure 3.9 DP and corresponding noise levels for 2f1− f2 low initial, after the introduction of the suppressor tone. Results represent an average across all 20 participants. Error bars represent one standard deviation. Absent = 0, Low = 20, med = 40, High = 60 dB SPL for the suppressor levels.

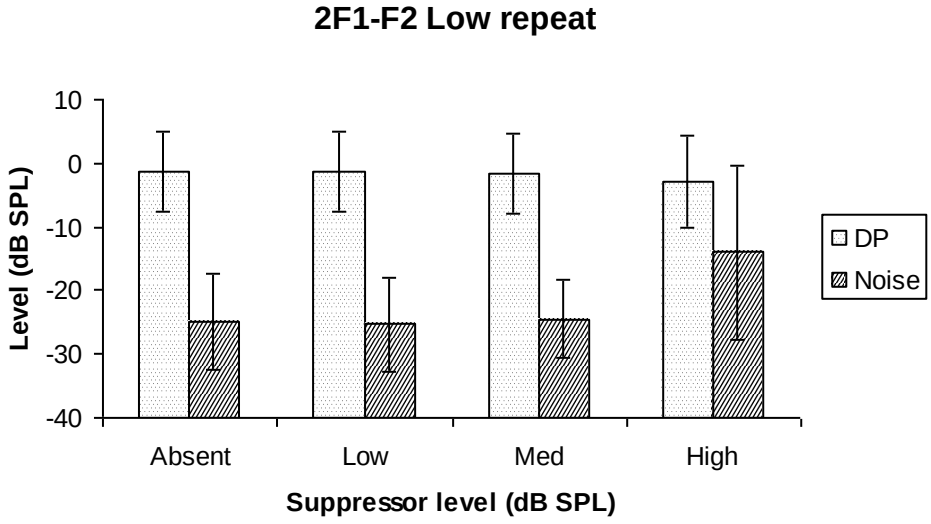

Figure 3.10 DP and corresponding noise levels for 2f1− f2 low repeat, after the introduction of the suppressor tone. Results represent an average across all 20 participants. Error bars represent one standard deviation. Absent = 0, Low = 20, med = 40, High = 60 dB SPL for the suppressor levels.

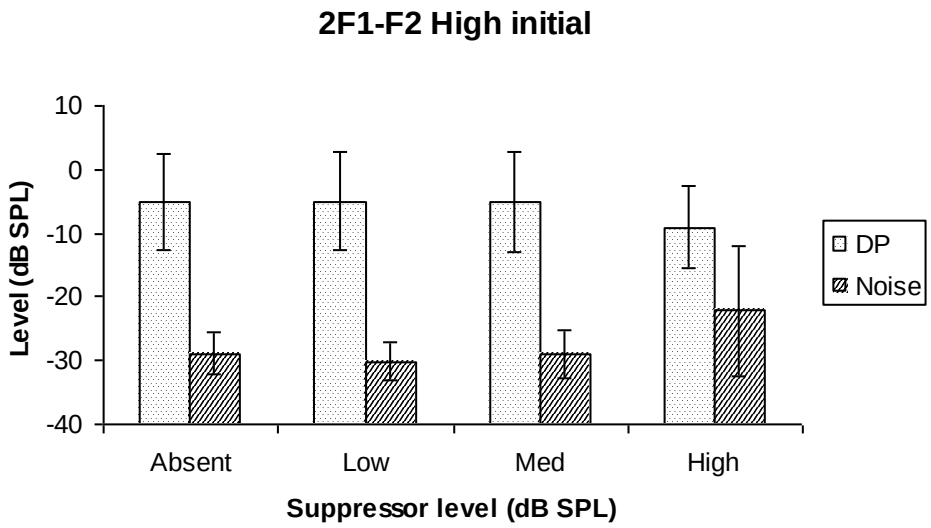

Figure 3.11 DP and corresponding noise levels for 2f1− f2 high initial, after the introduction of the suppressor tone. Results represent an average across all 20 participants. Error bars represent one standard deviation. Absent = 0, Low = 20, med = 40, High = 60 dB SPL for the suppressor levels.

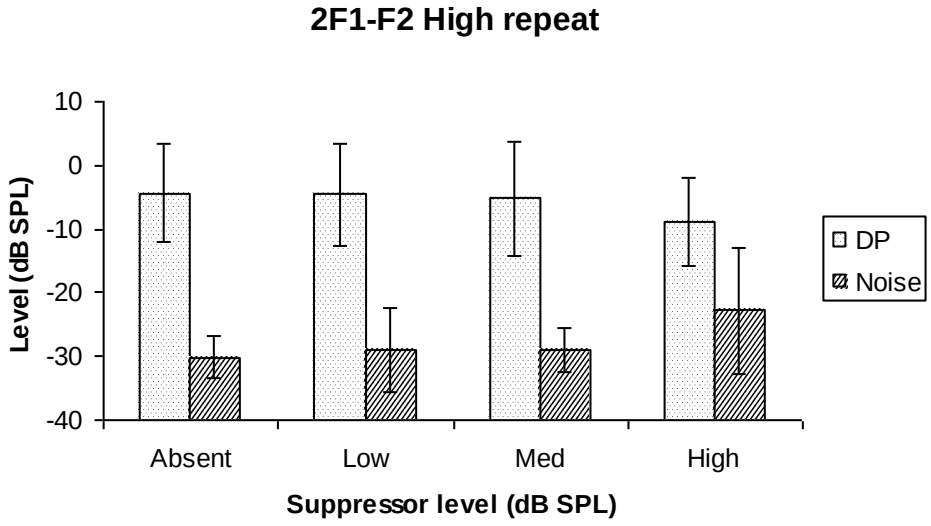

Figure 3.12 DP and corresponding noise levels for 2f1− f2 high repeat, after the introduction of the suppressor tone. Results represent an average across all 20 participants. Error bars represent one standard deviation. Absent = 0, Low = 20, med = 40, High = 60 dB SPL for the suppressor levels.

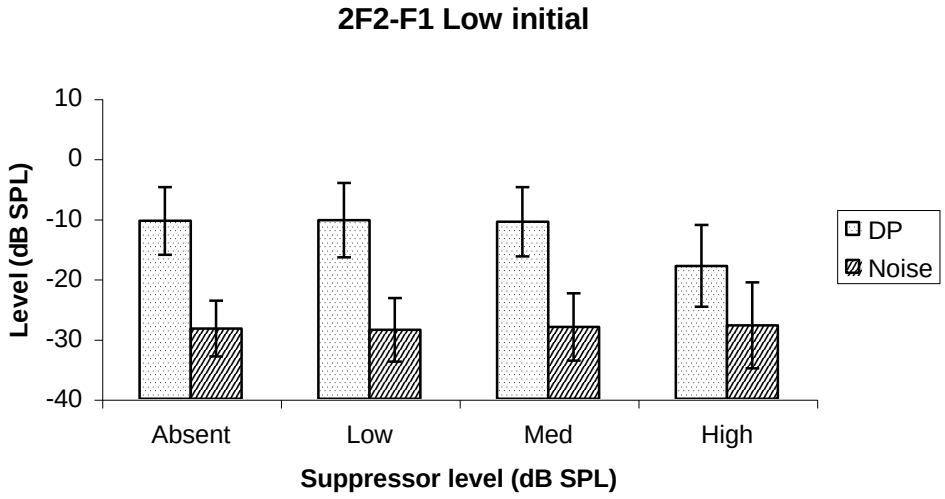

Figure 3.13 DP and corresponding noise levels for 2f2– f1 low initial, after the introduction of the suppressor tone. Results represent an average across all 20 participants. Error bars represent one standard deviation. Absent = 0, Low = 20, med = 40, High = 60 dB SPL for the suppressor levels.

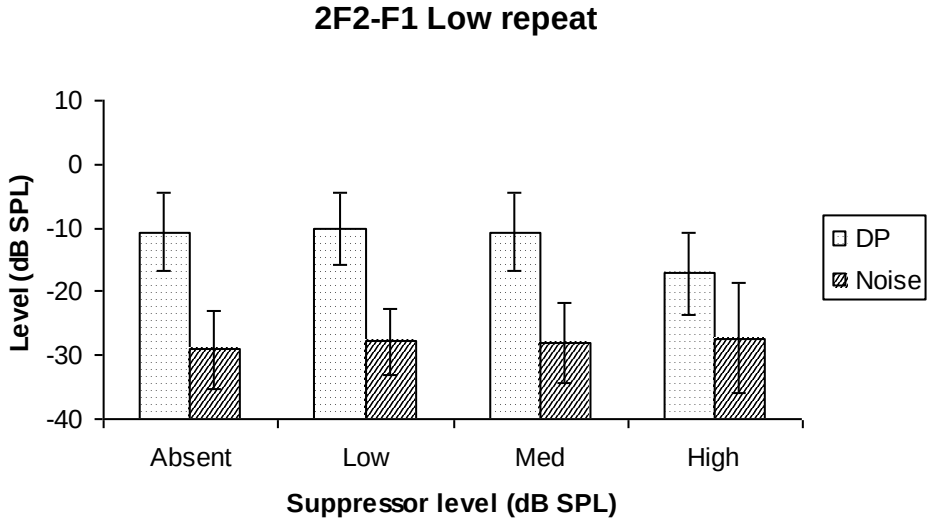

Figure 3.14 DP and corresponding noise levels for 2f2– f1 low initial, after the introduction of the suppressor tone. Results represent an average across all 20 participants. Error bars represent one standard deviation. Absent = 0, Low = 20, med = 40, High = 60 dB SPL for the suppressor levels.

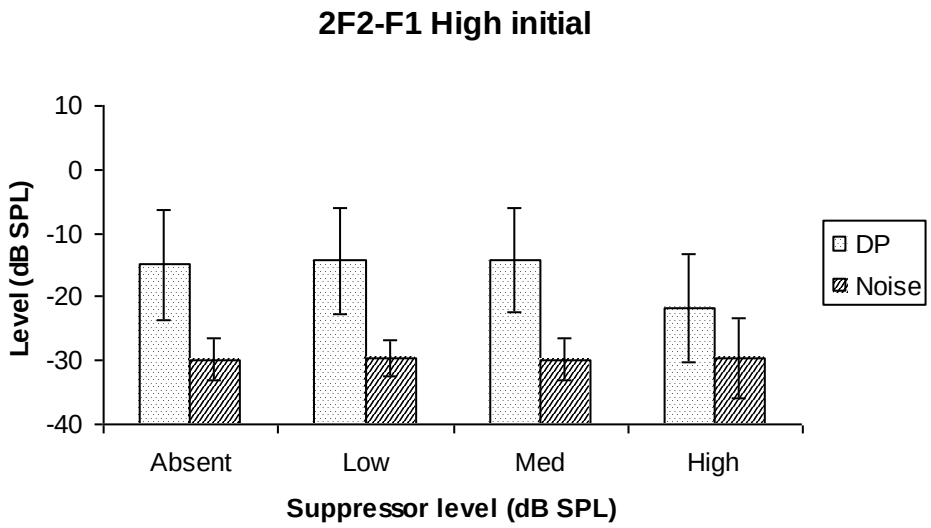

Figure 3.15 DP and corresponding noise levels for 2f2− f1 high initial, after the introduction of the suppressor tone. Results represent an average across all 20 participants. Error bars represent one standard deviation. Absent = 0, Low = 20, med = 40, High = 60 dB SPL for the suppressor levels.

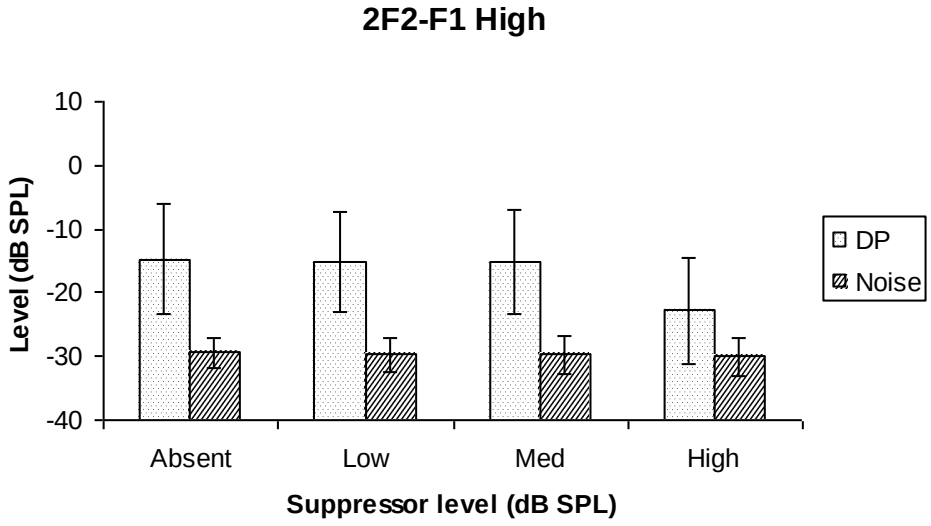

Figure 3.16 DP and corresponding noise levels for 2f2− f1 high repeat, after the introduction of the suppressor tone. Results represent an average across all 20 participants. Error bars represent one standard deviation. Absent = 0, Low = 20, med = 40, High = 60 dB SPL for the suppressor levels.

3.2.3 Individual results

In order to determine whether the DP level was significantly above the noise it is important not only to analyse the averaged data but also the individual participants. This is due to the potential for large variation between participants. Sharp (2007) and Wilson (2005) used a criterion of a minimum of a 3 dB difference between the DP level and the noise, to categorise if a DP is sufficiently present for each recording paradigm. The results of each individual are shown in Table 3.1 and it describes whether a sufficient signal is present or not. It is clear from the table that lower emission levels were exhibited for the 2f2− f1 low and high distortion components, with averages of 60 and 57.5 % present respectively.

Table 3.1 Individual participant data displaying the number of participants with DP levels 3 dB greater than the simultaneous noise levels.

Condition	Number recorded	Number present	% Present
2F1-F2 Low distortion initial	20	17	85
2F1-F2 Low distortion repeat	19	17	89
2F1-F2 Low reflection initial	20	20	100
2F1-F2 Low reflection repeat	19	19	100
2F1-F2 High distortion initial	20	20	100
2F1-F2 High distortion repeat	19	19	100
2F1-F2 High reflection initial	20	20	100
2F1-F2 High reflection repeat	19	19	100
2F2-F1 Low distortion initial	20	13	65
2F2-F1 Low distortion repeat	20	11	55
2F2-F1 Low reflection initial	20	20	100
2F2-F1 Low reflection repeat	20	19	95
2F2-F1 High distortion initial	20	11	55
2F2-F1 High distortion repeat	20	12	60
2F2-F1 High reflection initial	20	20	100
2F2-F1 High reflection repeat	20	20	100

3.2.4 Suppression-growth functions

Typical results demonstrating the effect of the different suppressor levels on the 2f1− f2 and 2f2− f1 high and low conditions are shown in Figures 3.17-3.20. These figures are presented in a format similar to those presented by Gaskill and Brown (1996) and Kummer et al. (1999). The figures show a downward trend in DP level with suppressor level across all conditions toward the high suppressor level. Each line in the figures shows the DPOAE level as a function of an increasing suppressor tone. These may be referred to as suppression-growth functions. Common characteristics of participants DP suppression were visible in each case. Figures 3.17-3.20 use data collected from participant SEL to exemplify these characteristics.

The level of suppression was largest under the high suppressor levels condition, as highlighted by the steep, parallel suppressor growth functions between the medium and high suppressor levels. As an example, Figure 3.17 (2f1− f2 low), with suppressor frequency of 1632 when no suppressor was introduced DP level was 4.7 dB, at 20 dB suppressor level the DP was at 4.1 dB, at 40 dB suppressor level the DP was 4.3 dB, and at 60 dB suppression the DP was 1.4 dB.

It must be noted that where occasional erroneous results were present they were omitted from the analysis. These points were only found for the 2f1− f2 low condition for the high suppressor level, and occurred infrequently in eight of the participants.

There was no visible effect of suppressor frequency on either the 2f1− f2 or 2f2− f1 condition.

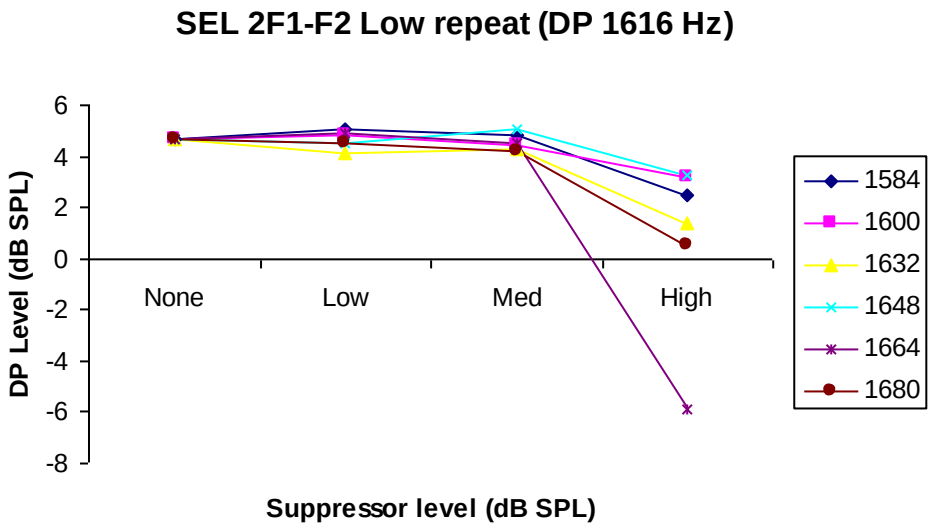

Figure 3.17 Level of DP as a function of suppressor level. The different lines represent different suppressor frequencies. The figure represents the 2f1– f2 low repeat DP at 1616 Hz condition for participant SEL. L1=65, L2=55, L1/L2=1.05. Suppressor levels were none, low, medium and high corresponding to 0, 20, 40, and 60 dB SPL respectively. Mean noise floor was –19.33 (±7.66 to one standard deviation) dB SPL.

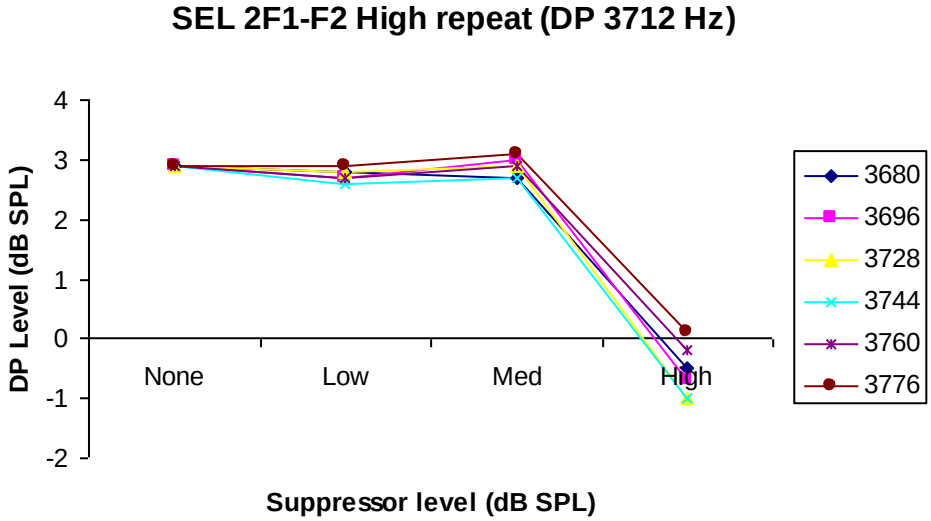

Figure 3.18 Level of DP as a function of suppressor level. The different lines represent different suppressor frequencies. The figure represents the 2f1– f2 high repeat DP at 3712 Hz condition for participant SEL. L1=65, L2=55, L1/L2=1.05. Suppressor levels were none, low, medium and high corresponding

to 0, 20, 40, and 60 dB SPL respectively. Mean noise floor was –25.73 (±6.56 to one standard deviation) dB SPL.

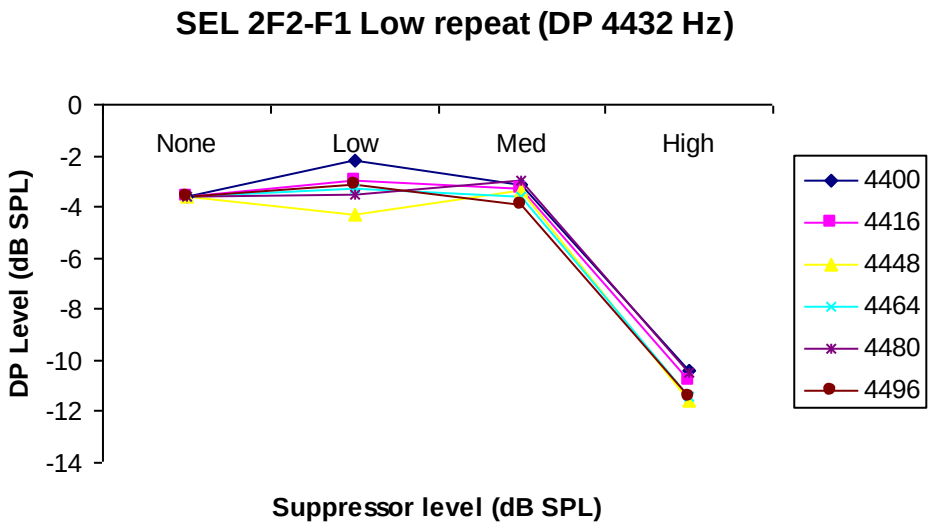

Figure 3.19 Level of DP as a function of suppressor level. The different lines represent different suppressor frequencies. The figure represents the 2f2– f1 low repeat DP at 4432 Hz condition for participant SEL. L1=65, L2=55, L1/L2=1.05. Suppressor levels were none, low, medium and high corresponding to 0, 20, 40, and 60 dB SPL respectively. Mean noise floor was –26.94 (±4.46 to one standard deviation) dB SPL.

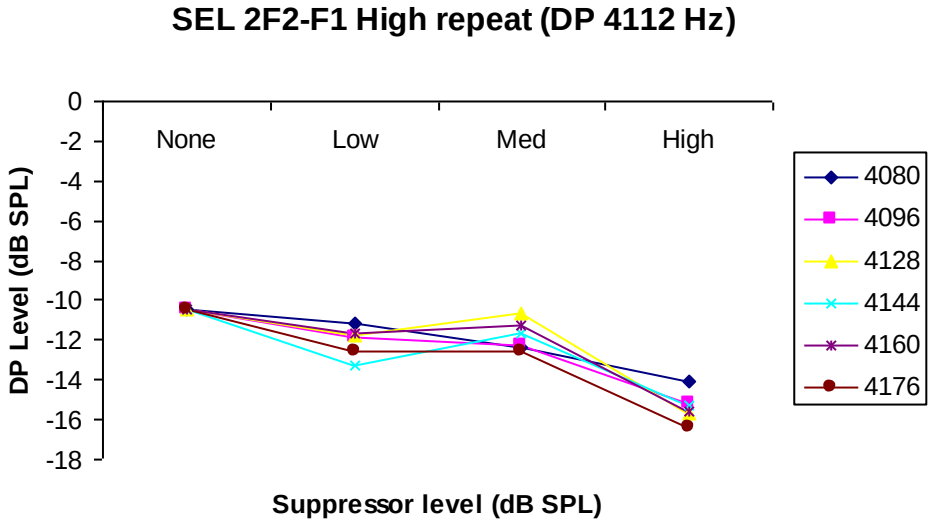

Figure 3.20 Level of DP as a function of suppressor level. The different lines represent different suppressor frequencies. The figure represents the 2f2– f1 high repeat DP at 4112 Hz condition for participant SEL. L1=65, L2=55, L1/L2=1.05. Suppressor levels were none, low, medium and high corresponding to 0, 20, 40, and 60 dB SPL respectively. Mean noise floor was –28.88 (±2.25 to one standard deviation) dB SPL.

3.3 Statistical interpretation

3.3.1 Patterns in the data

The DP and noise levels obtained from each participant were analysed in order to determine whether the data exhibited a normal distribution. Kolmogorov-Smirnov tests of normality were performed on the noise and DP levels of all participants under each experimental condition. Data was analysed for normality across both results for suppressor position and for suppressor level.

Of the 40 graphs produced (16 for suppressor level, 24 for suppressor position) 39 were normally distributed ($p > 0.05$) and one was not normally distributed ($p < 0.05$). This not normally distributed condition was:

DP	Placement	Variable
2f2-f1	High	Suppressor position (-16 Hz)

The results of the Kolmogorov-Smirnov tests suggest the underlying data distributions are approximately normal. Parametric testing was conducted throughout.

3.3.2 DP level compared to noise

The first hypothesis to be resolved determines if the DP recordings can be distinguished from the noise recordings. In order to resolve this dependent-means t-

tests were performed for each recording condition to further assess if the DP levels were significantly above the noise.

Considering the results for the paired t-tests it was clear that on average the participants experienced greater DP levels than noise levels.

For the 2f1− f2 low condition, participants experienced greater levels of DP (M = –1.33, SE = 0.78 dB SPL) when compared to noise (M = –25.29, SE = 0.47 dB SPL). This represents a significant difference $t(59) = -30.38$, $p < 0.05$.

This was true for the 2f1− f2 high condition with greater DP levels (M = –4.9, SE = 0.98 dB SPL) compared to noise (M = –29.29, SE = 0.28 dB SPL), $t(59) = -27.56$, $p < 0.05$.

This was also true for the 2f2− f1 low condition with greater DP (M = –10.42, SE = 0.07 dB SPL) than noise (M = –28.31, SE = 0.44 dB SPL), $t(59) = -29.83$, $p < 0.05$.

This also was true for 2f2− f1 high with a larger DP (M = –14.79, SE = 1.01 dB SPL) than noise (M = –29.69, SE = 0.25 dB SPL), $t(59) = -16.68$, $p < 0.05$.

Confidence intervals were also calculated via the t-test, which represents the SNR. The lowest lower limit was –26.16 dB SPL (2f1− f2 high) and highest upper was –13.12 dB SPL (2f2− f1 high).

Pearson's correlations coefficient was also calculated in order to determine if the larger DP levels were from those participants exhibiting the larger noise values. For all conditions the DP and noise levels demonstrated a significant correlation. For the 2f1-f2 low condition $r = 0.273$, $p < 0.05$, for 2f1-f2 high $r = 0.457$, $p < 0.05$, for 2f2-f1 low $r = 0.562$, and for the 2f2-f1 high condition $r = 0.576$, $p < 0.05$.

3.3.3 Analysis of variance (ANOVA)

It is important to note that for the 2f1− f2 low condition, for the high suppressor level, occasionally erroneous results were obtained. These results were clear outliers and removed, as described previously, before any further analysis.

An amplitude plot demonstrating the effect of suppressor position and level on the DP under the 2f1− f2 low condition is shown in Figure 3.21. The figure is averaged (mean) across all participants, and includes both the initial and repeat measurements. It is clear from the figure that initially the rise in suppressor level has little impact on the degree of suppression. However, the high suppressor level has a large effect on the DP level. The effect of suppressor frequency is not entirely clear.

Mauchly's test indicated that the assumption of sphericity had been violated for the main effects of suppressor level, c^2 (0.178), $p<0.05$, suppressor frequency, c^2 (0.029), $p<0.05$. Therefore degrees of freedom were corrected using Greenhouse-Geisser estimate of sphericity (for the main effect of suppressor level $\varepsilon = 0.612$, for the main effect of suppressor frequency $\varepsilon = 0.440$). The results of the two-way repeated ANOVA suggest a main effect of suppressor level, ($F_{1.8, 20.1} = 0.000$, $p<0.05$, $r = 0.94$.), but no effect of suppressor frequency ($F_{2.2, 24.2} = 0.204$, $p>0.05$). There was no significant interaction between suppressor level and suppressor frequency ($F_{2.5, 27.9} = 0.97$, $p>0.05$). Bonferroni post hoc test revealed a significant difference in DP levels between the high suppressor condition and the absent condition (CI95% = -3.937 lower, –1.594 upper, $p<0.05$), low condition (CI95% = –3.615 lower, –1.635 upper, $p<0.05$), and medium (CI95% = –3.652 lower, –1.673 upper, $p<0.05$). No other comparisons were significant ($ps>0.05$).

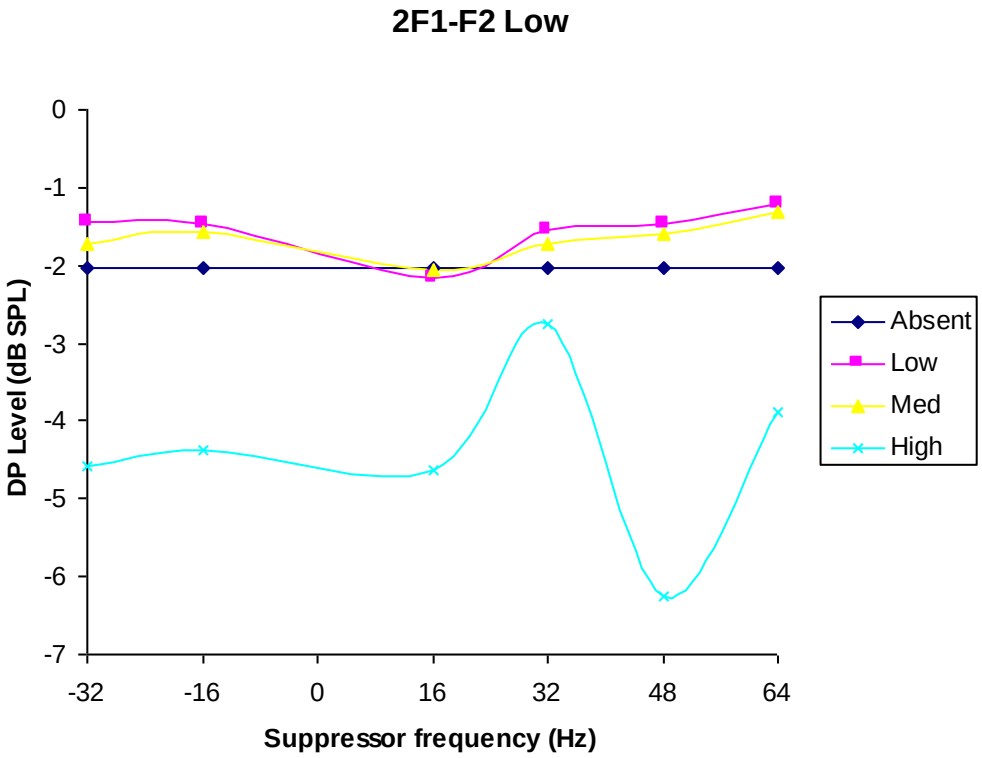

Figure 3.21 Amplitude plot of the 2f1− f2 low averaged across all 20 participants. The curves for suppressor levels are highlighted on the right-hand side of the plot. L1 = 65, L2 = 55, L1/L2 = 1.05. Absent suppressor level represents 0 dB SPL, Low represents 20 dB SPL, Medium represents 40 dB SPL, and High represents 60 dB SPL. Mean noise floor was –21.63 (±5.47 to one standard deviation) dB SPL. The 0 value on the x-axis represents the DP position. Outliers have been removed. The suppressor frequency represents the suppressor frequency relative to the DP.

An amplitude plot demonstrating the effect of suppressor frequency and level on the DP under the 2f1− f2 high condition is shown in Figure 3.22. The figure is averaged (mean) across all participants, and includes both the initial and repeat measurements. It is clear from the figure that the initial effect of increasing the suppressor level is noticeable, but not large. As the suppressor level increases there is a larger reduction in the DP level. The suppressor frequency appears to have little effect on the DP.

Mauchly's test indicated that the assumption of sphericity had been violated for the main effects of suppressor level, c^2 (0.117), $p<0.05$, suppressor frequency, c^2 (0.000),

p<0.05. Therefore degrees of freedom were corrected using Greenhouse-Geisser estimate of sphericity (for the main effect of suppressor level ε=0.584, for the main effect of suppressor frequency ε = 0.229). The results of the two-way repeated ANOVA suggest a main effect of suppressor level, ($F_{1.7, 64.7}$ = 0.000, P<0.05, r = 0.96), but no effect of suppressor frequency ($F_{1.1, 42.4}$ = 0.737, p>0.05). There was no significant effect between suppressor level and suppressor frequency ($F_{2.6, 97.0}$=0.533, P>0.05). Bonferroni post hoc testing revealed a significant difference in DP levels between the high suppressor condition and absent condition (CI95% = –5.439 lower, –3.168 upper, p<0.05), low (CI95% = –5.280 lower, –3.178 upper, p<0.05), and medium (CI95% = –5.109 lower, –2.654 upper, p<0.05). No other comparisons were significant (ps>0.05).

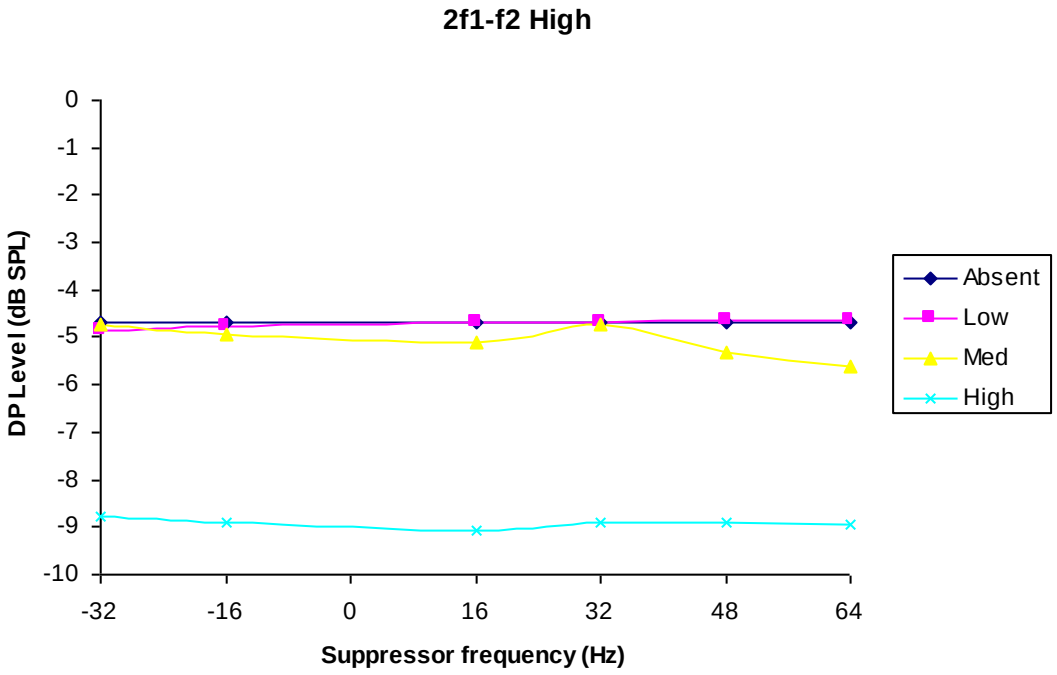

Figure 3.22 Amplitude plot of the 2f1– f2 high averaged across all 20 participants. The curves for suppressor levels are highlighted on the right-hand side of the plot. L1 = 65, L2 = 55, L1/L2 = 1.05. Absent suppressor level represents 0 dB SPL, Low represents 20 dB SPL, Medium represents 40 dB SPL, and High represents 60 dB SPL. Mean noise floor was –27.04 (±3.99 to one standard deviation) dB SPL. The 0 value on the x-axis represents the DP

position. The suppressor frequency represents the suppressor frequency relative to the DP.

An amplitude plot demonstrating the effect of suppressor frequency and level on the DP under the 2f2− f1 low condition is shown in Figure 3.23. The figure is averaged (mean) across all participants, and includes both the initial and repeat measurements. It is clear from the figure that even the lowest level of suppressor has a large effect on the DP level. The effect is largest for the highest level of suppressor. The effect of suppressor frequency is also visible, with a deepening of amplitude fine structure before the DP frequency is reached, and rising thereafter.

Mauchly's test indicated that the assumption of sphericity had been violated for the main effects of suppressor level, c^2 (0.099), $p<0.05$, suppressor frequency, c^2 (0.001), $p<0.05$. Therefore degrees of freedom were corrected using Greenhouse-Geisser estimate of sphericity (for the main effect of suppressor level $\varepsilon = 0.445$, for the main effect of suppressor frequency $\varepsilon=0.265$). The results of the two-way repeated ANOVA suggest a main effect of suppressor level, ($F_{1.3, 50.7} = 0.000$, $P<0.05$, $r = 0.96$), and a main effect of suppressor frequency ($F_{1.3, 50.2} = 0.000$, $p<0.05$, $r = 0.74$). There was also a significant effect between suppressor level and suppressor frequency ($F_{4.9, 187.9} = 0.000$, $p<0.05$, $r = 0.24$). Bonferroni post hoc testing revealed a significant difference in DP levels between the high suppressor condition and the absent condition (CI95% = -10.164 lower, -5.466 upper, $p<0.05$), low condition (CI95% = –9.188 lower, –4.865 upper, $p<0.05$), and medium (CI95% = –8.843 lower, –4.460 upper, $p<0.05$). There was also a significant comparison between the low condition and absent (CI95% = 4.460 lower, 8.843 upper, $p<0.05$), and between the medium condition and absent (CI95% = –2.016 lower, –0.311 upper, $p<0.05$). No other comparisons were significant ($ps>0.05$).

Significant effects were also shown between suppressor frequency –16 and –32 (CI95% = –7.985 lower, -1.756 upper, $p<0.05$), +16 (CI95% = –7.820 lower, -1.666 upper, $p<0.05$), +32 (CI95% = –7.844 lower, –1.523 upper, $p<0.05$), +48 (CI95% = –7.812 lower, –1.298 upper, $p<0.05$) and +64 (CI95%= –7.893 lower, –1.533 upper, $p<0.05$). Bonferroni post hoc testing revealed a significant difference in DP levels

between the high suppressor condition and the absent condition (CI95% = –10.344 lower, –4.561 upper, p<0.05), low condition (CI95% = –9.911 lower, –5.185 upper, p<0.05), and medium condition (CI95% = –9.905 lower, –5.363 upper, p<0.05). No other comparisons were significant (ps>0.05).

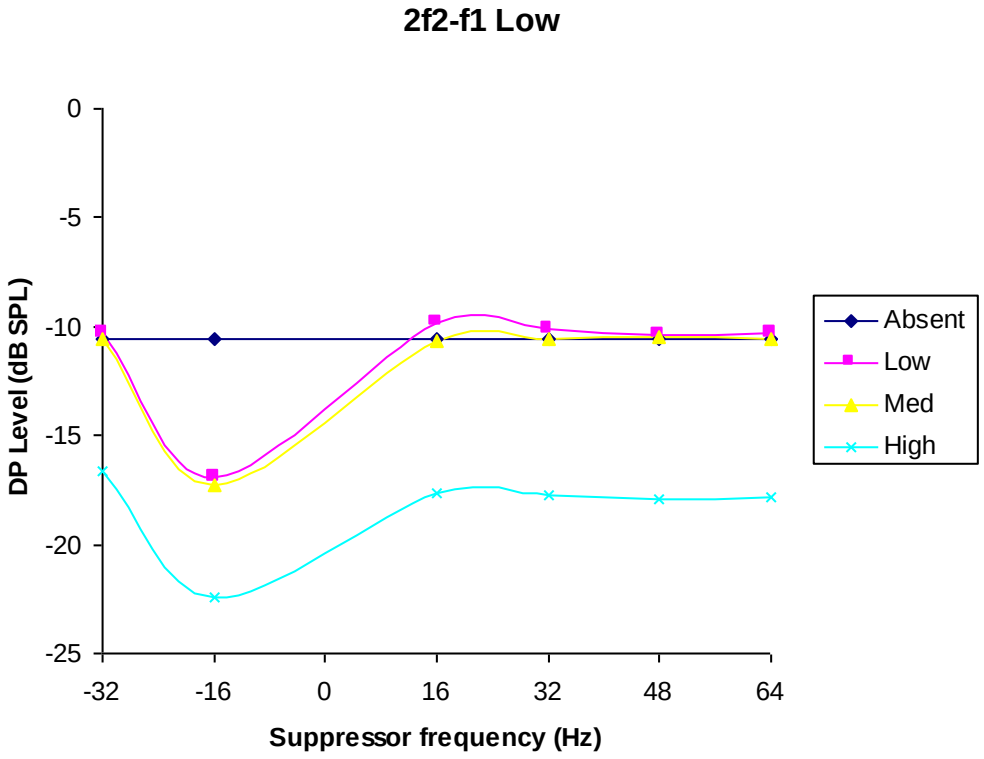

Figure 3.23 Amplitude plot of the 2f2– f1 low averaged across all 20 participants. The curves for suppressor levels are highlighted on the right-hand side of the plot. L1 = 65, L2 = 55, L1/L2 = 1.05. Absent suppressor level represents 0 dB SPL, Low represents 20 dB SPL, Medium represents 40 dB SPL, and High represents 60 dB SPL. Mean noise floor was –27.18 (±4.13 to one standard deviation). The 0 value on the x-axis represents the DP position. The suppressor frequency represents the suppressor frequency relative to the DP.

An amplitude plot demonstrating the effect of suppressor position and level on the DP under the 2f2– f1 high condition is shown in Figure 3.24. The figure is averaged (mean) across all participants, and includes both the initial and repeat measurements. The figure reveals that the suppressor initially has little effect. The DP actually rises initially for the low and medium suppressor levels, but declines for the highest

suppressor level. The effect of suppressor position for the low and medium position is that the DP level rises as the suppressor frequency approaches. For the high suppressor level as the suppressor frequency approaches the DP frequency there is a deepening in the amplitude fine structure, with an amplitude minimum exhibited after the DP frequency.

Mauchly's test indicated that the assumption of sphericity had been violated for the main effects of suppressor level, c^2 (0.056), $p<0.05$), suppressor frequency c^2 (0.465), $p<0.05$. Therefore degrees of freedom were corrected using Greenhouse-Geisser estimate of sphericity (for the main effect of suppressor level $\varepsilon = 0.463$, for the main effect of suppressor frequency $\varepsilon = 0.775$). The results of the two-way repeated ANOVA suggest a main effect of suppressor level, ($F_{1.3, 52.7} = 0.000$, $p<0.05$, $r = 0.95$), but no main effect of suppressor frequency ($F_{3.8, 147.3} = 0.694$, $p>0.05$). There was no significant effect between suppressor level and suppressor frequency ($F_{6.6, 252.0} = 0.192$, $p>0.05$).

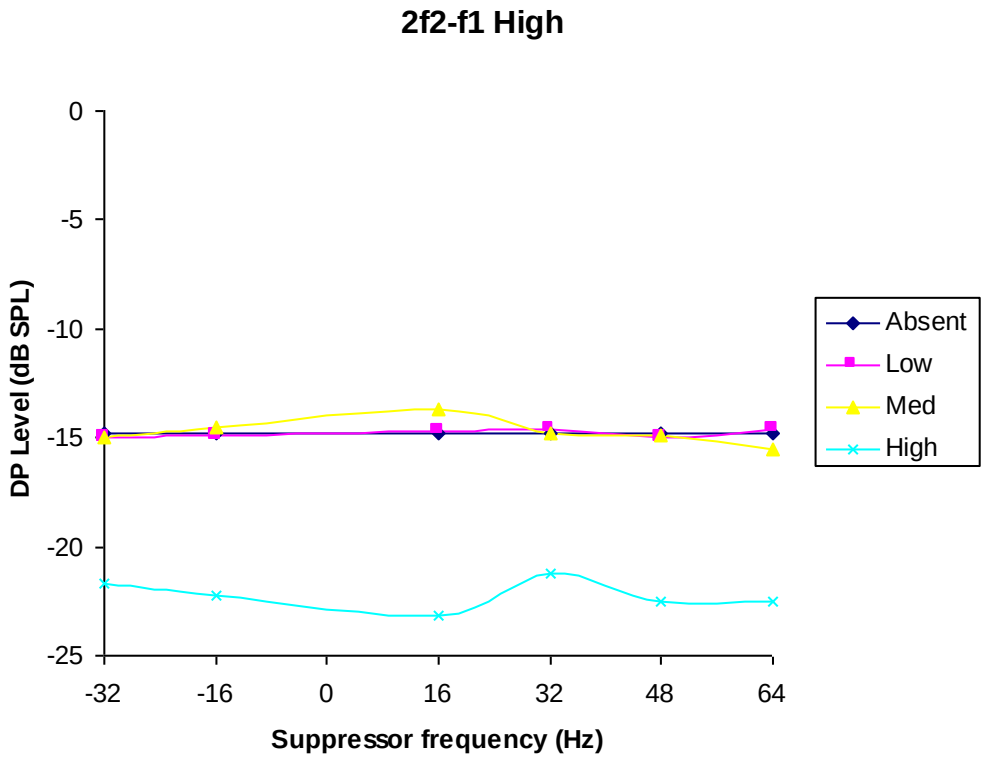

Figure 3.24 Amplitude plot of the 2f2– f1 high averaged across all 20 participants. The curves for suppressor levels are highlighted on the right-hand side of the plot. L1 = 65, L2 = 55, L1/L2 = 1.05. Absent suppressor level

represents 0 dB SPL, Low represents 20 dB SPL, Medium represents 40 dB SPL, and High represents 60 dB SPL. Mean noise floor was –29.77 (±2.16 to one standard deviation). The 0 value on the x-axis represents the DP position. The suppressor frequency represents the suppressor frequency relative to the DP.

CHAPTER 4: DISCUSSION

4.1 Introduction

Enhancing the understanding of the mechanisms of generation of OAEs is essential in utilising them to their full capacity in both the laboratory and clinic. Thus far, this paper has examined the literature surrounding the evolution of the models through which investigators have enhanced this understanding, particularly concerning DPOAEs. The physiological mechanisms underlying DPOAEs have been discussed (Shera, 2004; Robinette and Glattke, 2007), and methods of analysis have been described and criticised (Talmadge et al., 1999). The current two-source theory has been investigated, concerning the non-linear distortion and linear coherent reflection mechanisms (Shera and Guinan, 1999; Kalluri and Shera, 2001).

Two separation techniques have been described including time-window separation (Knight and Kemp, 2000) and the introduction of a suppressor tone (Maurmann et al., 1999; Gaskill and Brown, 1996). The paper emphasised present gaps in the understanding of DPOAEs, with particular reference to the 2f2− f1 DP.

The following questions were constructed:

- Is the 2f2− f1 DP is accurately measurable above the noise floor?
- What is the effect of suppressor level on the 2f2− f1 DP?
- What is the effect of suppressor frequency on the 2f2− f1 DP?

A methodology has been detailed and implemented in order to broaden understanding of this DP, and the results presented.

In this next section the results presented in the previous chapter will be discussed, along with how they relate to current understanding.

4.2 A question of validity and SNR

The results presented for the time window separation data support the theory that the parameters and conditions of measurement recording were valid, as the results are fully consistent with those of other investigators.

The IFFT output is similar to that demonstrated by Knight and Kemp (2000) with a peak seen below approximately 3 ms, followed by further peaks after. Knight and Kemp (2000) report that with a frequency ratio of f2− f1 = 1.04 the group delay was 3-4 ms, when using a frequency ratio of 1.2 the group delay was 0.5-1 ms. The peak with the small group delay signifies the wave-fixed emission, and the larger group delay reflects the place-fixed emission (Knight and Kemp, 2000).

It is clear from Fig 3.4 that the DP could be separated into two components typical of those shown by Kalluri and Shera (2001), and Shera (2004), and supported further by Wilson and Lutman (2006). The DP can be seen to be separating into two components, one with a phase not being influenced by frequency, and the others phase varying more with frequency. The original (unmixed) recording is similar to the reflection component, indicating predominance of that component, which is typically found for such frequency ratios.

The validity of the methodology implemented is further supported by the high SNRs obtained for the data both pre and post processing as exemplified in Figures 3.5-3.8. This emphasises that the parameters used (frequency ratio and primary levels) were sufficient to elicit recognisable responses. This further supports the results and methodology of Wilson and Lutman (2006) who found adequate SNRs for both the 2f1− f2 and 2f2− f1 emissions. Similar to these authors however, the 2f2− f1 DPs were lower than the 2f1− f2, particularly the distortion component. There is some overlap between the error bars of the noise and the DP. The results presented here are similar to those of Martin et al. (1998) and Wable et al. (1996) who also report that the amplitude of the 2f2− f1 DP is typically much lower than the 2f1− f2 DP.

After the introduction of the suppressor tone the results altered. These differences are exhibited under the high suppressor condition for both the 2f1− f2 and 2f2− f1 DPs.

This is potentially due to the effect the high suppressor level may have had on the recordings. As the suppressor was being delivered through the same channel as f1 it may have caused this higher apparent noise effect.

The results of the paired t-tests support the results displayed in the figures, as the DP levels were significantly above the noise in all cases.

However the validity of the results may be compromised by the significant correlation between the DP levels and the noise levels. The participants with the highest levels of DP had the highest levels of noise. This is perhaps due to the suppressor energy leaking into the FFT bins used for noise estimation, or inter-modulation with the suppressor increasing energy in these bins.

Further evidence supporting the validity of the results comes from the fact that all measurements were repeated. Both the initial and repeated measurements were very comparable to each other, almost being identical for both the 2f1− f2 and 2f2− f1 conditions, as shown in Figures 3.5-3.8.

All participants were given clear instructions to remain as still as possible throughout recording, and told to relax as much as possible. The participants were seated in a sound treated booth. This helped to achieve the lowest possible noise levels during the testing, protecting against noise contamination. This ensured the good SNR reported. This is an improvement over Knight and Kemps work (2001) who did not utilise completely sound treated conditions for the implementation of their methodology.

Further validity was acquired due to the large number of participants recruited. Often in DPOAE investigations the participant numbers are very low. Knight and Kemp (2001) for example only used the left ears of two participants; Talmadge et al. (1999) and Kalluri and Shera (2001) only used four participants. These low participant numbers may not be adequate to make accurate inferences.

It is important to note when discussing validity the apparently erroneous results, which were occasionally exhibited under the 2f1− f2 low conditions, when the high

suppressor level was in use. There are a number of issues that surround the use of a suppressor tone, as mentioned in Chapter 1. The suppressor may alter the response (Gorga et al., 2002), including having the potential to add more distortion sources. These newly created distortion products may leak into frequency bands utilised for the measurement of noise levels. The third tone may also have an additive effect on the measured DP, potentially leading to an increased DP level. Also discussed earlier is the problem of incomplete un-mixing, because of the inherent trade off between introducing the third tone at a level that is either too low or too high.
The large, overlapping error bars for the high suppressor level exhibited in Figures 3.9-3.16 reflect this. The apparently erroneous results were removed prior to further analysis. The results of the present investigation may be considered valid, as they are comparable to other investigations of a similar type, such as Sharp et al. (2007).

4.3 Suppression-growth functions

As an introduced suppressor tone increases in level it will at first not have a noticeable effect on the components of the DP (Talmadge et al., 1999). As the suppressor tone is initially introduced at a low level the DP level exhibits at first a stable plateau. As the suppressor level rises this stable period is followed by a rapid decline in DP level (Gaskill and Brown, 1996).

The results presented in the previous chapter support the experimental findings of previous investigations, such as those conducted by Gaskill and Brown (1996) and Kummer et al. (1995). The results presented here indicate that the 2f2− f1 DP can be suppressed in a similar way to the 2f1− f2 DP, for the experimental conditions utilised.

Kummer et al. (1995) reported that the location of the suppressor relative to the DP had a noticeable effect on the extent of suppression. The threshold of suppression was marginal approximately above f2 and minimally increased with raising frequency, but increased continuously with decreasing the level of the suppressor. Kummer et al. (1995) state that the DP was especially influenced by the suppressor

near to the DP frequency. The effect of suppressor frequency was not so evident here, potentially due to the different parameters utilised.

4.4 Amplitude plots

The ANOVA results expressed the significant effect of suppressor level on the DP for all conditions. For each condition there was a significant difference between the high suppressor condition and the absent condition. This is shown in the amplitude plots in Figures 3.21-3.24.

The amplitude plots in Figures 3.21-3.24 are exhibited in a similar fashion to those of Talmadge et al. (1999). Talmadge et al. (1999) introduced a third tone to determine the effect of level and position on the DP. The authors describe how in instances in which the reflection component is less than the non-linear distortion component increasing the level of the suppressor removes the amplitude fine structure. For cases in which the reflection component is greater than the non-linear distortion component increasing the suppressor level has the initial effect of making the reflection component equal to the non-linear distortion component, resulting in a deepening of the amplitude fine structure. When the suppressor level is large enough the reflection component becomes less than the non-linear distortion component and the amplitude fine structure disappears. For larger suppressor levels both the levels of the reflection and non-linear distortion component decrease, and there is a decline in the overall level of the DP (Talmadge et al., 1999). This provides further support for the two-source theory.

It has been demonstrated that for the recording parameters utilised in this investigation the reflection component is larger than the non-linear distortion component (Figures 3.5-3.8). It is expected that the results presented here could show similar results to those of Talmadge et al. (1999) for the condition under which the reflection component is larger than the non-linear distortion component. However, the deepening in the fine structure was only shown for the 2f2− f1 low condition. Figure 3.23 shows a deepening of amplitude fine structure as the suppressor frequency approaches the DP frequency, but then increasing. In Figures 3.21, 3.22 and 3.24 it is difficult to determine a discernible pattern at the high suppressor level.

In the amplitude plots only for the 2f2− f1 low condition was there a deepening in amplitude fine structure. For all other conditions this was not the case. This may imply support for the theory of Wilson and Lutman (2006), with the non-linear distortion and linear coherent reflection components arising from the DP frequency place.

4.4 The 2f2-f1 DP

The 2f2− f1 DP has been studied much less than the 2f1− f2 DP. It has been demonstrated on many occasions that the origin of the 2f2-f1 DP is basal to the DP frequency place along the BM (Wilson and Lutman, 2006; Erminy et al., 1998; Wable et al., 1996). Amplitudes are also reportedly lower for the 2f2− f1 DP in comparison to the 2f1− f2 DP (Wable et al., 1996). This is consistent with results of the current investigation as the 2f1-f2 is consistently larger than the 2f2− f1, and is located further above the noise floor. This is clear from figures 3.1-3.2. Moulin and Kemp (1996) implied this potentially is due to the DP not having the same location of generation as the 2f1− f2.

Knight and Kemp (2000) investigated the wave-fixed and place-fixed theory by using 2f1− f2 and 2f2− f1 DP stimulus frequency sweep data. Knight and Kemp (2000) discovered that there is a systematic change in the proportion of wave and place-fixed emissions. In the 2f1− f2 portion a wide stimulus frequency ratio results in wave-fixed emissions, whilst all other DPs are place-fixed. A transition occurs in this portion at f2/f1 = 1.1. This provided evidence that the mechanisms underlying the origin of 2f2− f1 and 2f1− f2 at lower frequencies ratios are fundamentally the same, but at greater frequency ratios there is an alternate source for the 2f1− f2 DP. Knight and Kemp (2000) suggest that these findings support the model that for wave-fixed emissions DP energy is largely created in the f2 region and is emitted directly. For other DPs even though the DP is generated due to the non-linearity within the f2 envelope, the DP is emitted by a combination of non-linearity and a reflection mechanism.

Knight and Kemp (2001) suggest that for the 2f1− f2 wave-fixed emission the DP originates in the f2 region and is emitted directly. All other DPOAEs are described by Knight and Kemp (2000) as place fixed, and the DP is not directly emitted but moves apically, where it is re-emitted basally as a consequence of a reflection mechanism. Knight and Kemp (2001) document that in one of their two participants (RN) both a wave-fixed and place-fixed component in the 2f2− f1 DP was exhibited, but could not define it as being a normal characteristic as it was only located above the noise in a single participant. Knight and Kemp (2001) report that the origins are potentially in the region of the DP frequency place in the cochlea.

Wilson and Lutman (2006) investigated the wave and place-fixed components of the 2f1− f2 and 2f2− f1 emission, to determine if it was a common feature of human ears. The authors used frequency ratios f2/f1 of 1.05, 1.1, 1.22, and 1.32. They did indeed discover that both wave and place-fixed components were present in most of the participants (emissions present in all but two place-fixed 2f2− f1 DP recordings). Wilson and Lutman (2006) proposed a mechanism of generation of the 2f2− f1 DP, which can be seen in Figure 1.11. Waves of the primary frequencies f1 and f2 travelling past the 2f2− f1 DP place are basal to the characteristic frequency so subsequently are not slowed by the mechanics of the cochlea. It is suggested that non-linearity at the 2f2− f1 DP place results in energy being emitted basally through a reverse TW or through the cochlear fluids. Wilson and Lutman (2006) conclude that it may be assumed that the non-linear distortion and the linear coherent reflection components occur at the DP frequency place, or basal to it.

The investigation described here offers support for the theory of Wilson and Lutman (2006), as it was not possible to selectively suppress the reflection or distortion component of the DP separately. This points towards a distributed source of the distortion mechanism, at or basal to the DP frequency place.

Martin et al. (1998) used suppression, onset latencies and correlation techniques to further examine the generation site of the 2f2− f1 DP compared to the 2f1-f2 DP. Martin et al. (1998) conclude that the 2f2− f1 DPOAE is generated at, or basal to, the 2f2− f1 frequency place.

Sharp (2007) further investigated the components of the 2f1− f2 and 2f2− f1 by not only using a time window separation method, but also a suppression technique. Sharp (2007) utilised the same four frequency ratios as Wilson and Lutman (2006). The investigation revealed that both the 2f1− f2 and the 2f2− f1 DPOAEs exhibit wave and place-fixed components, when subject to both suppression and time window separation techniques. The DPOAEs found by Sharp (2007) by both methods exhibited similar patterns, with only the wave-fixed component of 2f1− f2 having a high dependence on frequency ratio. The levels of the different DPOAE components did alter greatly between the two methods, highlighting large variations in the results of the two techniques. Sharp (2007) concludes that as it was possible to separate the distortion and reflection components of the 2f1− f2 and 2f2− f1 emission via suppression, they must arise by similar mechanisms. Sharp (2007) suggested that the position of the suppressor relative to the DPs may have an influence on the possible levels of suppression. Placing the suppressor between the DP and the primaries may have increased the efficacy of the suppressor.

The suppressor method works based on the different locations of generation of the two different components. If the two components were originating from the same place of origin, then the suppression method would not be able to separate the two components, as suggested by Wilson and Lutman (2006). This investigation revealed that the introduction of a suppressor tone does indeed reduce the overall levels of the DP for both the 2f1− f2 and 2f2− f1, but in most cases it was not possible to selectively suppress either component separately. As the suppressor technique is dependent on the generation sites being physically remote, it can be assumed that the origins of the 2f2− f1 emission, unlike those of the 2f1− f2 emission are not separated spatially.

The evidence presented in this investigation supports the theory of Wilson and Lutman (2006) that for the 2f2− f1 DP potentially the reflection and distortion sources are at an identical location on the BM.

4.5 Future work

It has been noted that delivering a suppressor tone through the same channel as one of the primaries may result in possible interaction between the two stimuli, which complicates interpretation. It was attempted in this study to deliver the suppressor tone through a third channel using a REM probe tube. However, it was not possible to obtain sufficiently accurate synchronisation with the primaries to satisfy the requirements of the recording technique. In a future experiment it would be interesting to deliver the third tone through a separate channel, if possible, to more accurately assess the effect of a third tone on the DP.

There is still very little literature concerning the origins of the 2f2− f1 DP. It would be interesting to further validate the experimental findings of this investigation but utilising a wider range of frequency ratios. Here the frequency ratio 1.05 was used. It would be valuable to further determine if similar results are obtained for other frequency ratios such as 1.1 and 1.22. Also by using a larger number of suppressor frequencies, relative to the DP, including possibly multiple suppressors, a more complete picture of the effect of suppressor position on the DP level can be established.

5. Conclusion

It is clear that both the non-linear distortion and reflection component of the 2f1− f2 and 2f2− f1 can be measured above the noise floor when separated by time-windowing. Time window separation is a technique that relies on the different latencies of the components.

Suppression analysis revealed that at low levels of suppression there is a minimal effect on the DP levels. At higher suppression levels there is a decline in the overall level of the DP.

No effect of suppressor frequency was revealed.

It was not possible to separate the two components of the 2f2− f1 DP by suppression, a technique that relies on location. This may imply a distributed source of the distortion mechanism, at or basal to the DP frequency place.

References

Abdala, C. (2005). Effects of aspirin on distortion product otoacoustic emission suppression in human adults: A comparison with neonatal data. *J. Acoust. Soc. Am.* **118**: 1566-1575.

Avan, P., & Bonfils, P. (1993). Frequency specificity of human distortion product otoacoustic emissions. *Audiology* **32**: 12-26.

Avan, P., Magnan, P., Smurzynski, J., Probst, R., & Dancer, A. (1998). Direct evidence of cubic difference tone propagation by intracochlear acoustic pressure measurements in the guinea-pig. *European Journal of Neuroscience* **10**: 1764-1770.

Boege, P. & Janssen, T. (2002). Pure-tone threshold estimation from extrapolated distortion product otoacoustic emission I/O-functions in normal and cochlear hearing loss ears. *J. Acoust. Soc. Am.* **111**: 1810-1818.

Brown, A.M., Harris, F.P., & Beveridge, H.A. (1996). Two sources of acoustic distortion products from the human cochlea. *J. Acoust. Soc. Am.* **100**: 3260-3267.

British Society of Audiology (1992). Recommended procedure for tympanometry. *British Journal of Audiology*, **26**: 255-257.

British Society of Audiology (2004). Pure tone air and bone conduction threshold audiometry with and without masking and determination of uncomfortable loudness levels.

British Society of Audiology (2010). Recommended procedure: Ear examination.

Cheatham, M.A., Huynh, K.H., Gao, J., Zuo, J., & Dallos, P. (2004). Cochlear function in prestin knockout mice. *J Physiol.* **560**: 821-830.

Cheatham, M.A., Zheng, J., Huynh, K.H., Du, G.G., Gao, J., Zuo, J., Navarrete, E., & Dallos, P. (2005). Cochlear function in mice with only one copy of the prestin gene. *J Physiol*. **569**: 229-241.

Dallos, P. (1992). The active cochlea. *The Journal of Neuroscience* **12**: 4575-4585.

Dhooge, I., Dhooge, C., Geukens, S., De Clerck, B., De Vel, E. and Vinck, B.M. (2006). Distortion product otoacoustic emissions: An objective technique for the screening of hearing loss in children treated with platin derivatives. *International Journal of Audiology,* **45**: 337-343.

Dorn, P.A., Konrad-Martin, D., Neely, S.T., Keefe, D.H., Cyr, E., & Gorga, M.P. (2001). Distortion product otoacoustic emission input/output functions in normal-hearing and hearing-impaired human ears. *J. Acoust. Soc. Am*. **110**: 3119-3131.

Duke, T., & Julicher, F. (2003). Active travelling wave in the cochlea. *PhysRevLett.* **90**: 8101.

Emadi, G., Richter C.P., & Dallos, P. (2004). Stiffness of the gerbil basilar membrane: Radial and longitudinal variations. *J Neurophysiol* **91**: 474-488.

Erminy, M., Avan, P. and Bonfils, P. (1998). Charachteristics of the acoustic distortion product 2f2-f1 from the normal human ear. *Acta Otolaryngol (Stockh)* **118**: 32-36.

Field, A. (2009). *Discovering Statistics Using SPSS*. Third Edition. London: Sage Publications Ltd.

Gaskill, S.A., & Brown, A.M. (1990). The behaviour of the acoustic distortion product, 2f1-f2, from the human ear and its relation to auditory sensitivity. *J. Acoust. Soc. Am.* **88**: 821-839.

Gaskill, S.A., & Brown, A.M. (1993). Comparing the level of the acoustic distortion product 2f1-f2 with behavioural threshold audiograms from normal-hearing and hearing-impaired ears. *British Journal of Audiology* **27**: 397-407.

Gelfand, S.A. (2007). *Hearing – An Introduction to Psychological and Physiological Acoustics.* 4th Edition. New York: Informa Healthcare.

Gorga, M.P., Neely, S.T., Dorn, P.A., Dierking, D. and Cyr, E. (2002). Evidence of upward spread of suppression in DPOAE measurements. *J. Acoust. Soc. Am.* **112**: 2910-2920.

Hammershoi, D., & Moller, H. (1996). Sound transmission to and within the human ear canal. *J. Acoust. Soc. Am.* **100**: 408-427.

He, N., & Schmiedt, R.A. (1997). Fine structure of the 2f1-f2 acoustic distortion product: Effects of primary level and frequency ratios. *J. Acoust. Soc. Am.* **101**: 3554-3565.

Janssen, T., Boege, P., Oestreicher, E. and Arnold, W. (2000). Tinnitus and 2f1-f2 distortion product otoacoustic emissions following salicylate overdose. *J. Acoust. Soc. Am.* **107**: 1790-1792.

Kalluri, R., & Shera, C.A. (2001). Distortion-product source unmixing: A test of the two-mechanism model for DPOAE generation. *J. Acoust. Soc. Am.* **109**: 622-637.

Kemp, D.T. (2002). Otoacoustic emissions, their origin in cochlear function, and use. *British Medica Bulletin* **63**: 223-241.

Kemp, D.T., Ryan, S., & Bray, P. (1990). A guide to the effective use of otoacoustic emissions. *Ear and Hearing* **11**: 93-105.

Kimberley, B.P., Hernadi, I., Lee., A.M., & Brown, D.K. (1994). Predicting pure tone thresholds in normal and hearing-impaired ears with distortion product emission and age. *Ear & Hearing* **15**: 199-209.

Knight, R.D., & Kemp, D.T. (2000). Indications of different distortion product otoacoustic emission mechanisms from a detailed f1,f2 area study. *J. Acoust. Soc. Am.* **107**: 457:473.

Knight, R.D., & Kemp, D.T. (2001). Wave and place fixed DPOAE maps of the human ear. *J. Acoust. Soc. Am.* **109**: 1513-1525.

Konrad-Martin, D., Neely, S.T., Keefe, D.H., Dorn, P.A., & Gorga, M.P. (2001). Sources of distortion product otoacoustic emissions revealed by suppression experiments and inverse fast Fourier transforms in normal ears. *J. Acoust. Soc. Am.* **109**: 2862-2879.

Kummer, P., Janssen, T., & Arnold, W. (1995). Suppression tuning characteristics of the 2f1-f2 distortion product otoacoustic emission in humans, *J. Acoust. Soc. Am.* **98**: 197-210.

Kummer, P., Janssen, T., & Arnold, W. (1998). The level and growth behaviour of the 2f1-f2 distortion product otoacoustic emission and its relationship to auditory sensitivity in normal hearing and cochlear hearing loss. *J. Acoust. Soc. Am.* **103**: 3431-3444.

Liberman, M.C., Zuo, J., & Guinan, J.J. (2004). Otoacoustic emissions without somatic motility: Can stereocilia mechanics drive the mammalian cochlear? *J. Acoust. Soc. Am.* **116**: 1649-1655.

Lonsbury-Martin, B., Cutler, W.M., & Martin, G.K. (1991). Evidence for the influence of aging on distortion-product otoacoustic emissions in humans. *J. Acoust. Soc. Am.* **89**: 1749-1759.

Martin, G.K., Jassir, D., Stagner, B.B., and Whitehead, M.L. (1998). Locus of generation for the 2f1-f2 vs 2f2-f1 distortion-product otoacoustic emissions in

normal-hearing humans revealed by suppression tuning, onset latencies, and amplitude correlations. *J. Acoust. Soc. Am.* **103**: 1957-1971.

Mauermann, M., Uppenkamp, S., van Hengel, P.W.J., & Kollmeier, B. (1999). Evidence for the distortion product frequency place as a source of distortion product otoacoustic emission (DPOAE) fine structure in humans. I. Fine structure and higher-order DPOAE as a function of the frequency ratio f2/f1. *J. Acoust. Soc. Am.* **106**: 3473-3483.

Miller, J.A.L., & Marshall, L. (2001). Monitoring the effects of noise with otoacoustic emissions. *Seminars in Hearing* **22**: 393-403.

Moulin, A. and Kemp, D.T. (1996). Multicomponent acoustic distortion product otoacoustic emission phase in humans. II. Implications for distortion product otoacoustic emissions generation. *J. Acoust. Soc. Am* **100**: 1640-1662.

Oeken, J., Lenk, A., & Bootz, F. (2000). Influence of age and presbyacusis on DPOAE. *Acta oto-Laryngologica*, **120**: 396-403.

Olson, E.S. (1999). Direct measurement of intra-cochlear pressure waves. *Nature* **42**: 526-529.

Osterhammel, P.A., Rasmussen, A.N., Olsen, S.O., & Nielsen, L.H. (1996). The influence of spontaneous otoacoustic emissions on the amplitude of transient-evoked emissions. *Scand Audiol* **25**: 187-92.

Oxenham, A.J., & Shera, C.A. (2003). Estimates of human cochlear tuning at low levels using forward and simultaneous masking. *JARO* **4**: 541-554.

Ren, T. (2004). Reverse propagation of sound in the gerbil cochlea. *Nature Neuroscience* **7**: 333-334.

Ren, T., & Gillespie, P.G. (2007). A mechanism for active hearing. *Current Opinion in Neurobiology* **17**: 498-503.

Ren, T., He, W., Scott, M., & Nuttall, A.L. (2006). Group delay of acoustic emissions in the ear. *J Neurophysiol* **96**: 2785-2791.

Robinette, M.S., Glattke, T.J. (2007). *Otoacoustic Emissions- Clinical Applications*. 3rd Edition. New York: Thieme.

Robles, L., & Ruggero, M.A. (2001). Mechanics of the mammalian cochlea. *Physiol Rev* **81**: 1305-1352.

Robles, L., Ruggero, M.A., & Rich, N.C. (1997). Two-tone distortion on the basilar membrane of the chinchilla cochlea. *J Neurophysiol* **77**: 2385-2399.

Ruggero, M.A. (2004). Comparison of group delays of 2f1-f2 distortion product otoacoustic emissions and cochlear travel times. *Acoust Res Lett Online* **5**: 143-147.

Shaffer, L.A., Withnell, R.H., Dhar, S., Lilly, D.J., Goodman, S.S., & Harmon, K.M. (2003). Sources and mechanisms of DPOAE generation: Implications for the prediction of auditory sensitivity. *Ear & Hearing* **24**: 367-379.

Sharp, J.S. (2007). *Wave-fixed and place-fixed sources of distortion product otoacoustic emissions*. MSc Dissertation, Faculty of Engineering, Science and Mathematics. Institute of Sound and Vibration Research. University of Southmapton.

Shera, C.A. (2004). Mechanisms of mammalian otoacoustic emission and their implications for the clinical utility of otoacoustic emissions. *Ear and Hearing* **25**:86-97.

Shera, C.A., & Guinan, Jr., J.J. (1999). Evoked otoacoustic emissions arise by two fundamentally different mechanisms: A taxonomy for mammalian OAEs. *J. Acoust. Soc. Am.* **105**: 782-798.

Shera, C.A., & Zweig, G. (1993). Noninvasive measurement of the cochlear travelling-wave ratio. *J. Acoust. Soc. Am.* **93**: 3333-3352.

Shera, C.A., Talmadge, C.L., & Tubis, A. (2000). Interrelations among distortion-product phase-gradient delays: Their connection to scaling symmetry and its breaking. *J. Acoust. Soc. Am.* **108**: 2933-2948.

Siegel, J.H., Cerka, A.J., Recio-Spinoso, A., Temchin, A.N., van Dijk, P., & Ruggero, M.A. (2005). Delays of stimulus-frequency otoacoustic emissions and cochlear vibrations contradict the theory of coherent reflection filtering. *J. Acoust. Soc. Am.* **118**: 2434-2443.

Suckfull, M., Schneeweiss, Dreher, A., & Schorn, K. (1996). Evaluation of TEOAE and DPOAE measurements for the assessment of auditory thresholds in sensorineural hearing loss. *Acta Octolaryngol (Stockh)* **116**: 528-533.

Sun, X., Schmiedt, R.A., He, N., & Lam, C.F. (1994)[a]. Modeling the fine structure of the 2f1-f2 acoustic distortion product. I. Model development. *J. Acoust. Soc. Am.* **96**: 2166-2174.

Sun, X., Schmiedt, R.A., He, N., & Lam, C.F. (1994)[b]. Modeling the fine structure of the 2f1-f2 acoustic distortion product. II. Model evaluation. *J. Acoust. Soc. Am.* **96**: 2175-2183.

Talmadge, C.L., Long, G.L., Tubis, A., & Dhar, S. (1998). Experimental confirmation of the two-source interference model for the fine structure of distortion product otoacoustic emissions. *J. Acoust. Soc. Am.* **105**: 275-292.

Talmadge, C.L., Tubis, A., Long, G.R., & Piskorski, P. (1998). Modeling otoacoustic emission and hearing threshold fine structures. *J. Acoust. Soc. Am.* **104**: 1517-1543.

van Dijk, P., & Manley, G.A. (2001). Distortion product otoacoustic emissions in the tree frog *Hyla cinerea*. *Hearing Research* **153**: 14-22.

Wable, J., Collet., L. and Chery-Croze. S. (1996). Phase delay measurements of distortion product otoacoustic emissions at 2f1-f2 and 2f2-f1 in human ears. *J. Acoust. Soc. Am.* **100**: 2228-2235.

Wilson, H.K. (2005). *Wave-fixed and place-fixed sources of distortion product otoacoustic emissions*. MSc Dissertation, Faculty of Engineering, Science and Mathematics. Institute of Sound and Vibration Research. University of Southmapton.

Wilson, H.K. & Lutman, M.E. (2006). Mechanisms of generation of the 2f2-f1 distortion product otoacoustic emission in humans. *J. Acoust. Soc. Am.* **120**: 2108-2115.

Zhao, F. and Stephens, D. (1999). Test-retest variability of distortion-product otoacoustic emissions in human ears with normal hearing. *Scandanavian Audiology*, **28**: 171-178.

Zweig, G., & Shera, C.A. (1995). The origin of periodicity in the spectrum of evoked otoacoustic emissions. *J. Acoust. Soc. Am.* **98**: 2018-2047.

Appendices

Appendix 1

function [Dp_complex_eq, Dp_dist_amp, Dp_dist_nowind, Dp_ref_amp, Dp_ref_nowind, Dp_freq_eq] = unmixing(n, tcutoff, filename, f1, f2, Dp_type, Dp_amp, Dp_phase)

```
%function [Dp_complex_eq, Dp_dist_amp, Dp_dist_nowind, Dp_ref_amp,
Dp_ref_nowind, Dp_freq_eq] =
%         unmixing(n, tcutoff, filename, f1, f2, Dp_type, Dp_amp, Dp_phase)
%
%function of the unmixing algorithm according to Withnell et al Hear. Res. 178,
2003, 106-117
%input parameters:  n:order of the recursive exponential filter (try 10)
%               tcutoff: filter cutoff (recursive exponential filter) in ms
%               filename: name of input data file
%               Dp_type: coded DP 1=2f1-f2 and 2=2f2-f1
%               f1, f2: vectors of frequency values in sweep
%               Dp_amp, Dp_phase vectors of amplitude (dB) and phase values
%               in sweep from get_dp_file function called previously
%output parameters: Dp_complex_eq
%               Dp_dist_amp D component mag vector
%               Dp_dist_nowind D component vector without Hann window
%               Dp_ref_amp R component mag vector
%               Dp_ref_nowind R component vector without Hann window
%               Dp_freq_eq vector of DP frequencies
%-------------------------------------------------------------------------

fs=32768;
%sample frequency of the system (Hz)
deltaf=16;
%binwidth
N=fs/(deltaf);
%N number of points in frequency (2048 till fs no till Nyquist, no mirroring)
Max_freq=deltaf*N;
%max frequency (32768 hz according to the article you have to go till fs, no till
Nyquist)
f=[deltaf:deltaf:Max_freq/2];
%frequency vector till Nyquist
```

%step 1: conversion of Amplitude and Phase in complex number;Amplitude in mPa e Phase

```
%unwrapped in radians
Dp_amp_mPa=unitconv2(Dp_amp,'dBmPa');
Dp_phase_rad=Dp_phase*(pi/180);
Dp_phase_rad_unw=unwrap_local(Dp_phase_rad);       % unwrap function to avoid
jumps greater than pi
```

```
Dp_complex=complex(Dp_amp_mPa.*cos(Dp_phase_rad_unw),
Dp_amp_mPa.*sin(Dp_phase_rad_unw));
```

%step 2: linear interpolation of the data to obtain 16 Hz of step between the Dp frequency.

```
%With our way of recording we have a step of 32 or 16 Hz
if Dp_type == 1
   Dp_freq=2*f1-f2;
   xlabel_text='2f1-f2 (Hz)';
elseif Dp_type == 2
   Dp_freq=2*f2-f1;
   xlabel_text='2f2-f1 (Hz)';
else
   error('Unsupported DP type: must be 1 or 2')
end

random=rand(length(Dp_freq),1);
Dp_freq=(Dp_freq+random);
Dp_freq=sort(Dp_freq);
Dp_freq_eq=[Dp_freq(1):deltaf:Dp_freq(length(Dp_freq))];
Dp_complex_eq=interp1(Dp_freq,Dp_complex,Dp_freq_eq,'linear');
```

%step 3: the complex data is buffered with zeros from 0 to fs.

```
%No mirroring of the complex data is performed.
buffer_data=zeros(1,N);
index=fix(N*(Dp_freq_eq./Max_freq));
buffer_data(index)=Dp_complex_eq;
```

%step 4: perform IFFT.

```
%The time resolution is 30.5 micros. The time-domain waveform obtained from the
IFFT
%extended from 0 to 62.5 ms (2048 points multiplied by 30.5 micros).
time_nowind=ifft(buffer_data,N);            % analytic signal
time_nowind_magn=abs(time_nowind);          % envelope of the analytic signal
t=[0:(1/Max_freq):(N-1)*(1/Max_freq)].*1000;  % time vector (in ms!)
```

%step 5: IFFT is multiply by a n-order recursive exponential filter to remove %components attribute to reflections within the cochlea (developped by Shera and Zweig 1993)

```
rec_filt = recur_expo_filt(n,tcutoff,t);
filter_time=time_nowind.*rec_filt;                    %filter on time data
figure;plot(t,time_magn,'r',t,abs(filter_time));
title(strcat(' [', filename, ']'));
```

%step 6: An FFT is performed on filtered IFFT.

```
%The FFT is performed on N value but only the first 0 to N/2 values are necessary
(the
%values from N/2+1 to N-1 are redundant conjugates). The individual FFT are
summed to obtain
```

```
%the total FFT,i.e.the complex amplitude of the wave-fixed (or distortion)
component.
filtered_freqdata=fft(filtered_windowed_time,N,2);
Dp_dist_nowind=fft(filter_time,N);          %complex amplitude of the wave-fixed
component
Dp_dist_amp=unitconv2(abs(Dp_dist(index)),'mPadB');
Dp_dist_nowind_amp=unitconv2(abs(Dp_dist_nowind(index)),'mPadB');
Dp_eq_amp=unitconv2(abs(Dp_complex_eq),'mPadB');

%step 7: the total place-fixed (or reflection)component is obtained by
subtraction of the
%complex amplitude of the wave-fixed from the original data
Dp_ref_nowind=Dp_complex_eq-Dp_dist_nowind(index);
Dp_ref_amp=unitconv2(abs(Dp_ref),'mPadB');
Dp_ref_nowind_amp=unitconv2(abs(Dp_ref_nowind),'mPadB');

str1=strcat('Dp Amplitude', ' [', filename, ']');
str2=strcat('Dp Phase', ' [', filename, ']');
figure;subplot(2,1,1);
plot(Dp_freq_eq,Dp_eq_amp,'ro-',Dp_freq_eq, Dp_dist_nowind_amp,'gs-
',Dp_freq_eq,Dp_ref_nowind_amp,'bd-
',Dp_freq,Dp_amp,'k','LineWidth',1,'MarkerSize',2);
h=gca;set(h,'YLim',[-60 20]);title(str1);ylabel('dB SPL');
hold on;subplot(2,1,2);
plot(Dp_freq_eq,unwrap_local(angle(Dp_complex_eq)),'ro-
',Dp_freq_eq,unwrap_local(angle(Dp_dist_nowind(index))),'gs-
',Dp_freq_eq,unwrap_local(angle(Dp_ref_nowind)),'bd-
',Dp_freq,Dp_phase_rad_unw,'k','LineWidth',1,'MarkerSize',2);
h=gca;set(h,'YLim',[-40 10]);title(str2);ylabel('Radians');xlabel(xlabel_text);
legend('Dp','DpDis','DpRef','Original',3);

Dp_dist_nowind=Dp_dist_nowind(index);
% in this way all the vector exported have the same length.


function p = unwrap_local(p_in)
%LocalUnwrap   Unwraps row vector of phase values in radians
p=p_in;
m = length(p);
for i=2:m
  if (p(i)-p(i-1)) > pi
          for j=i:m
                  p(j) = p(j) - 2*pi;
          end
  end
end
```